Tribological and Machinability Performance of Hybrid Al2O3 -MWCNTs MQL for Milling Ti-6Al-4V

Muhammad Jamil (engr.jamil@nuaa.edu.cn)
Nanjing University of Aeronautics and Astronautics
Ning He
Nanjing University of Aeronautics and Astronautics
Wei Zhao
Nanjing University of Aeronautics and Astronautics
Aqib Mashood Khan
Nanjing University of Aeronautics and Astronautics
Munish Kumar Gupta
Shandong University

Research Article

Keywords: Cutting force, cutting temperature, chip analysis, surface integrity

Posted Date: June 1st, 2021

DOI: https://doi.org/10.21203/rs.3.rs-550038/v1

Tribological and machinability performance of hybrid Al_2O_3 -MWCNTs MQL for milling Ti-6Al-4V

Muhammad Jamil [a], Ning He [a], Wei Zhao [a,*], Aqib Mashood Khan [a], Munish Kumar Gupta [b],

[a] College of Mechanical and Electrical Engineering, Nanjing University of Aeronautics and Astronautics, Nanjing, 210016, China. Email: engr.jamil@nuaa.edu.cn; dr.aqib@nuaa.edu.cn; drnhe@nuaa.edu.cn ;

[b] Key Laboratory of High Efficiency and Clean Mechanical Manufacture, Ministry of Education, School of Mechanical Engineering, Shandong University, Jinan, PR China. Email: munishguptanit@gmail.com;

Corresponding authors: Wei Zhao Email: nuaazw@nuaa.edu.cn

Abstract: Recent burgeoning development in nanotechnology unfold an avenue in the manufacturing industry. Owing to the superior heat transfer potential of nanoadditives mentioned recently, it could be interesting to improve the heat transfer and tribological capability of metal cutting fluids by mixing nanofluids in emulsions properly. In order to attain high-performance cutting of difficult-to-cut alloys, hybrid nanofluids assisted Minimum Quantity Lubrication (MQL) system is applied with the anticipation of efficient lubrication and heat transfer. Taguchi based $L_{16}(4^3)$ orthogonal array is used involving nanofluids concentrations of alumina-multiwalled carbon nanotubes (Al_2O_3-MWCNTs) air pressure and cooling flow rate at constant cutting conditions in the milling of Ti-6Al-4V. The resultant cutting force (F_R), cutting temperature (T), and surface roughness (Ra) is considered as key machining responses. Besides, tool wear, chip analysis, and surface topography are also analyzed under the effect of hybrid nanofluids. Findings have shown the minimum resultant force, cutting temperature and surface roughness of 24.3N, 148.7^{o}C, and 0.67µm respectively at nanofluids concentration of 0.24vol%, 120ml/h of flow rate at 0.6MPa of air pressure. The microscopic analysis of the end-mill depicted minor thermal damage, chip-welding, and coating peeling. Also, chip analysis depicts the clean back surface and less melting of saw-tooth chip edges. The surface topography confirms the less micro-adhesion of chips and material debris. The summary showed that appropriately chosen MQL parameters have improved the lubrication/cooling performance by providing oil film and enhancing the milling performance measures. The outcomes of the proposed study are useful for the manufacturing industry for the enhancement of process performance.

Keywords: Cutting force; cutting temperature; chip analysis; surface integrity

1. Introduction:

Ti-6Al-4V (*α-β alloy*) has become an attractive alternative due to exceptional performance at high-temperature owing to strength, resistance to corrosion, and high toughness. That is why, it has enormous usage in shipbuilding, automobile, aerospace, and medical industries. Ti-6Al-4V is hard-to-cut, reactive to tool material at elevated temperature, prone to the built-up edge (BUE) formation, welding of chips during cutting, with a high coefficient of friction [1]. Thermal conductivity of Ti-6Al-4V is also extremely less (6.7W/mK), accumulates heat into the workpiece material leading to surface burning, fatigue, and thermal shock.

Surface burning leads to poor surface quality, and chemical reactivity accelerating the tool wear as reported by numerous researchers [2–4]. To cope up with the challenge, it is necessary to use low cutting conditions to achieve better surface quality, low temperature, and gradual tool wear. In the meantime, low cutting conditions reduce productivity, which is unacceptable from the industrial point of view. The application of mineral-based metal cutting fluids is very common in the industry to control the heat generation and to provide adequate lubrication. However, the emerging sustainable approach to reduce consumption of cutting fluids (i.e., 785 billion tons in 2018) [5], 15~17% of the coolant cost, and associated disposal cost have put forward to adopt dry or near-to-dry sustainable cooling techniques in machining.

A near to dry minimum quantity lubrication (MQL) is used to improve the machining characteristics during the process of medium-hard materials [6]. MQL reduced 40~60% of the lubrication cost, fluid quantity, and pressurized fine coolant spray to penetrate at the cutting zone effectively [6]. However, MQL effectiveness decreases significantly during machining of Ti-6Al-4V due to high heat generation during cutting. Due to the poor thermal conductivity, this heat accumulates at primary cutting zone enabling ease in reactivity towards cutting tool material, chip welding, and BUE formation that accelerates tool wear. The nickel-based superalloy was machined under MQL based CNC milling through uncoated carbide tools. A comparison between mineral and vegetable oil assisted MQL was applied at the varying flow rate, nozzle distance, nozzle type, and type of cutting process. The performance measures were tool life and cutting forces. The findings have indicated that vegetable oils provided extended tool life at a flow rate of 100 ml/h in up milling process [7]. In a nutshell, MQL has the potential to limit the heat generation, improve production quality and material removal rate. Considering the importance of improving the material removal rate in the industry, the addition of nanoparticles of 1-100nm size particles dispersed in vegetable oil-based MQL has been adopted widely to improve the lubrication and thermal conductivity of a nanofluid [8]. Numerous types of nanoparticles are available in the market for various applications such as iron oxide (Fe_2O_3), aluminum nitride (AlN), zinc oxide (ZnO), alumina (Al_2O_3), single, and multi-walled carbon

nanotubes (MWCNTs). The addition of a tiny volume of nano-additives in base oil significantly increases the surface area of cooling medium, heat transfer, and stable Brownian motion of particles [9,10]. The effect of MWCNTs assisted MQL in the machining of Ti-6Al-4V is investigated at varying cutting conditions. A significant decrease in surface roughness was observed due to the formation of stable tribological thin film and filled micro-pores on newly generated machined surface and the tool cutting edge [11]. Another study has considered the comprehensive comparison of silver and alumina nanoparticles assisted MQL in the machining of Nickle alloy. The comparison has provided exciting results about the turning performance measures. The alumina-based nanoparticles have provided less cutting force, wear, and chip curling due to small contact angle, fine droplet, and spreadability of particles. Besides, the exceptional ball-bearing effect of silver nanofluids provided good surface quality and limited abrasive wear [12]. Fig.1 depicts the critical advantages of the application of hybrid nanofluids, such as preventing the direct contact of the tool surface with the workpiece surface, filling the workpiece surfaces gaps, and transferring the heat from the workpiece to cutting fluids.

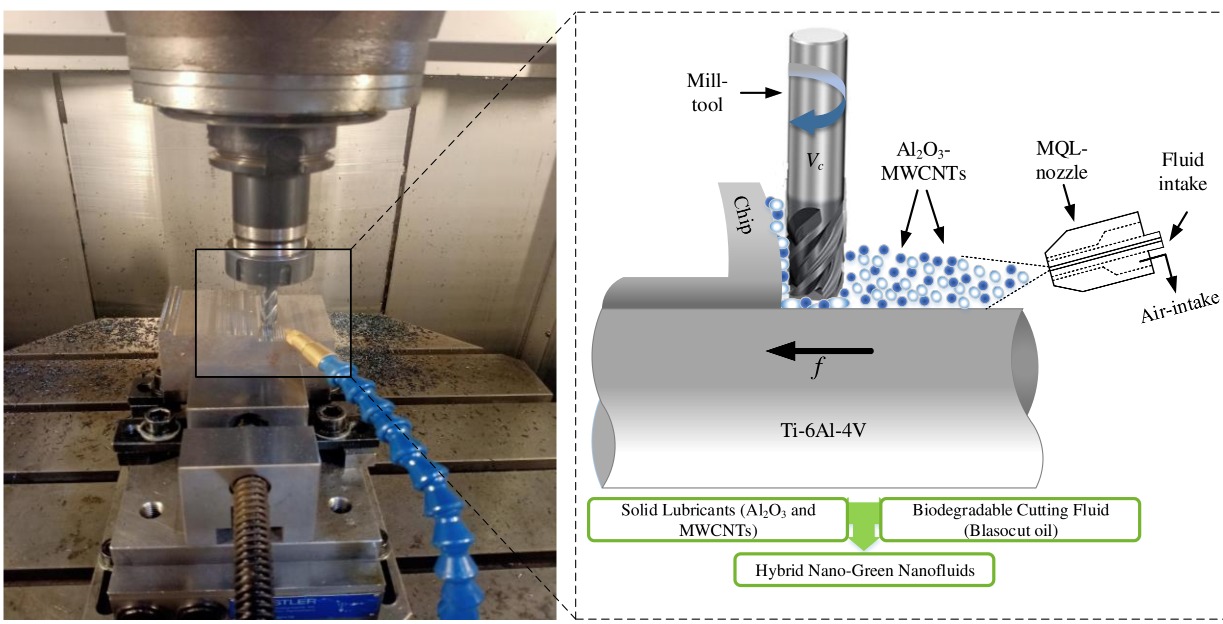

Figure 1: Application of hybrid nanofluids through the minimum quantity lubrication system

The application of hybrid nanoparticles based MQL has been reported more effective to provide better cooling/lubrication due to the synergistic effect of both particles. Ahammed et al., mixed Al_2O_3-graphene nanofluids and reported 88.62% increase in thermal conductivity and a 4.7% reduction in temperature in mini-channel heat exchangers [13]. An attempt has been made to investigate the Al_2O_3-MWCNTs hybrid nanofluids to evaluate the effect of temperature, surface roughness, and tool life in the machining of hard materials. The hybrid nanoparticles were dispersed in vegetable oil. Results have shown that hybrid nanofluids have improved surface finish by 8.72%, cutting force by 11.8% and tool life by 23% compared

to cryogenic-CO_2 cooling [14]. Similarly, Nine et al., have combined Al_2O_3-MWCNTs and reported an improvement in thermal conductivity [15]. Zhang et al. have applied MoS_2-MWCNTs in the grinding process and reported lower grinding ratio 'G' and surface roughness than individual mixed MoS_2 or MWCNTs nano-additives [16]. Furthermore, MWCNTs nanoadditives based MQL has been applied in the machining of titanium dispersed in vegetable oil in different concentrations to optimize the turning process. Results have concluded that 2 wt% MWCNTs reduced power by 11.5% compared to MQL without additives [17].

To improve the thermal and tribological characteristics of nanofluids, Al_2O_3-MWCNTs have been applied in different concentrations. The study showed a significant reduction in wear and friction coefficient due to excellent lubrication, wettability, and dispersion. Besides, hybrid nanofluids have reduced flank wear by 11%, and nodal temperature by 27.36% as compared to only Al_2O_3 based MQL cooling/lubrication [18]. The spherical shape Al_2O_3 nano-additives and cylindrical morphology of MWCNTs have different sizes, that can penetrate in-depth. In addition, MWCNTs have weak Van der Waal forces and easily shear under external load. A significant reduction of friction coefficient can also be associated with inter-tubular slip at the tool-chip interface. Thermal conductivity of MWCNTs is very high (3000~6000 W/m^{o}C) that dissipates heat, lower friction, and formation of tribo-layer on the workpiece surface that lowers the friction effect over-time period in machining. A recent study has discussed the tremendous advantages of 1.25 vol.% of hybrid nanofluids (Alumina-MWCNTs) regarding the cutting forces and surface roughness measurement. Authors have reported high thermal conductivity, viscosity, specific heat ratio, and relatively less density than only alumina or base fluids. Regarding the application of hybrid nanofluids in machining, 20% less main cutting force, and 33.4% less surface roughness have been mentioned compared to only Al_2O_3 nanofluids [19].

The principal objective of this research study is to investigate the effect of hybrid nanofluids dispersed in vegetable oil-based MQL parameters to model and optimize simultaneously the MQL associated parameters in milling of Ti-6Al-4V to improve the machinability. Taguchi based-L_{16} orthogonal array was applied to design the experiments. The fluid concentration, flow rate, and air pressure were varied to investigate their effect on cutting forces, temperature, and surface roughness.

2. Experimental Details

In this experimental study, milling experiments were performed on Ti-6Al-4V alloy under hybrid nanofluids based MQL technology. Besides, the effect of cutting conditions and concentration of fluid (wt.%), flow rate (mL/h), and pressure (MPa) are considered as critical parameters. The performance measures such as milling force, temperature, and surface quality were investigated under MQL technology.

2.1 Design of experiment

In order to investigate the performance of hybrid nanofluids under machining Ti-6Al-4V, constant cutting conditions of cutting speed (100 m/min), feed per tooth (0.02 mm/tooth), a width of cut (0.4 mm) and depth of cut (0.5 mm) were used through the experimentation to remove the uncertainty. The levels of the variable parameters were determined through a series of trial tests and recommendations from the tool manufacturer. The workpiece is Ti-6Al-4V alloy with dimensions of 150x80x50 mm^3 and is prepared for experimentation in Fig.2a. The EDS analysis was done on workpiece material to determine the elemental distribution Fig.2 (b).

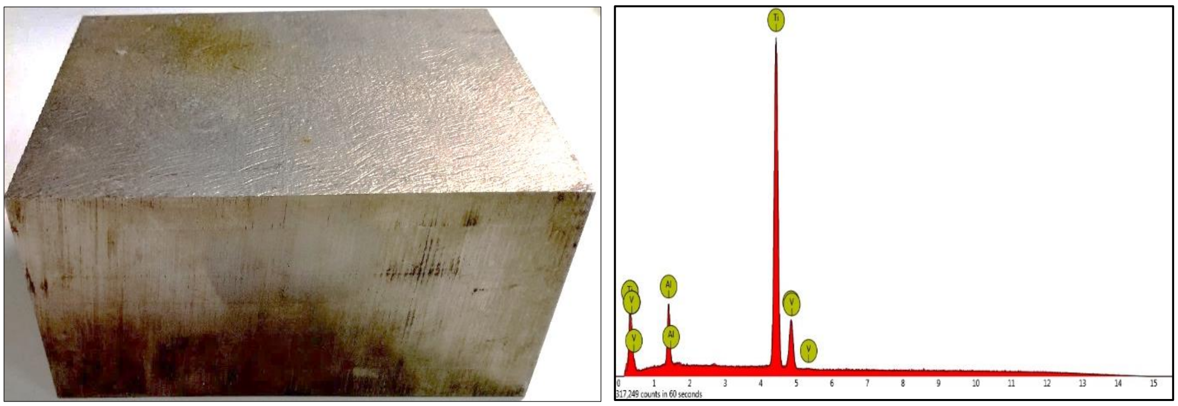

Figure 2: (a) The workpiece sample prepared for milling process (b) EDS analysis of the workpiece

Before experimental runs, the grinding process was performed to remove the outer oxide layer. The solution 20% and 5% of nitric acid and hydrofluoric acid were used to take off the layer of the heat-affected zone. The chemical composition and thermo-physical properties of Ti-6Al-4V are provided in Table 1.

Table 1:The chemical, mechanical and thermal characteristics of Ti-6Al-4V [17]

Chemical composition of Ti-6Al-4V							
Al	V	C	Fe	O	N	H	Ti
5.5-6.74%	3.5-4.5%	0.1%	0.3%	0.2%	0.05%	0.0125%	Balanced (%)

Thermo-mechanical properties of Ti-6Al-4V			
Density	4470 kg/m^3(at 23°C)	Yields Strength	828 MPa (0.2% offset)
Young's Modulus	114 GPa	Elongation	10%
Poisson's ratio	0.3 (at 23°C)	Hardness	30-34 Rc
Tensile strength	895 MPa	Specific heat	560 J/kgC
Thermal conductivity	7.2 W/m C	Melting point	1649 °C

The CNC milling (Model: Mikron UCP-710), having a maximum of 20,000 rotations per minute (RPM) and motor power of 13.4 kW, was used to perform the experiments. The cemented coated carbide cutting tools (Manufactured by Guhring; Types: 3629) are reported as ideal due to high hardness, toughness, wear-resistance, and excellent performance even at high temperatures [11]. The TiAlN coating was used due to high oxidation temperature and hardness, good thermal resistivity, and adhesion with poor frictional coefficient and thermal conductivity [20]. Fig.3 depicts the geometric characteristic of the end-mill showing helical length, total length, and helix angle features.

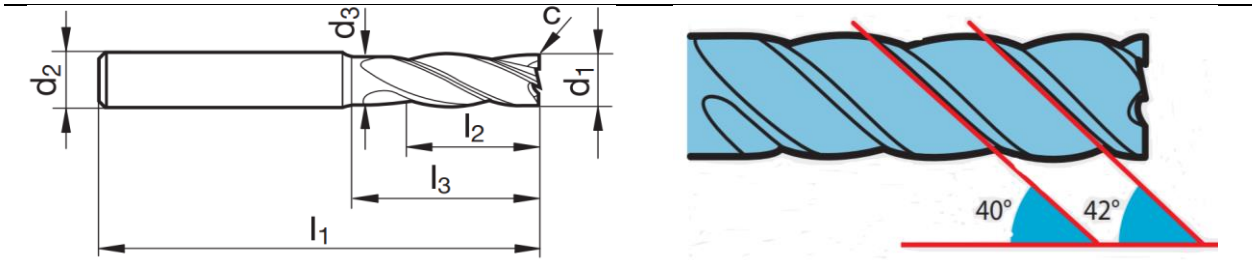

d1(mm) h10	d2(mm) h6	d3(mm)	I_1(mm)	I_2(mm)	I_3(mm)	C(mm×45°)	Z	Ø°	Hardness:
8	8	7.70	63	19.0	26.0	0.15	4	40~42	<1300 N/mm^2

Figure 3: The coated carbide power-mill with geometric characteristics

The variable machining conditions (hybrid nanofluids concentration, MQL flow rate, and compressed air pressure) are control factors. MQL flow rate was controlled by the MQL system, and constant air pressure was supplied by a compressor. Based on the number of parameters and levels, Taguchi based $L_{16}(4^3)$ orthogonal array is used to design of experiments. Design Expert 10.0.0 was used to design the experiments and to perform the analysis of variance (ANOVA), the significance of the model, and the contribution of each parameter. Parameters and their levels used for a total of 16 experimental runs (Table 2).

Table 2: The minimum quantity lubrication factors and levels

Variable name	Units	Parameter Levels			
		1	2	3	4
Nanofluids concentration (Conc.)	(wt.%)	0.06	0.12	0.18	0.24
MQL flow rate (f_r)	(mL/h)	40	80	120	160
Air pressure (A_p)	MPa	0.5	0.6	0.7	0.8

2.2 Hybrid nanofluids preparation and MQL system

Initially, Blasocut (Vascomill MMS FA-1, Blaser-Swisslube, Switzerland) oil having 5vol% of distilled water was used as base fluid. The hybrid Al_2O_3-MWCNTs is finally achieved by mixing 25% of

Al_2O_3 nanoadditives (diameter: 20~30 nm) with the multiwalled carbon nanotubes MWCNTs (diameter: 30~50nm) in 90:10 at different concentration in the base fluids. There was no surfactant or detergent used in this preparation of hybrid nanofluids, keeping the sustainability perspective during preparations. These nanofluids were ultrasonicated in Digital Ultrasonic heater for 3hrs to prepare stable and homogeneous suspension [18]. (Fig.4). The process was repeated in cycles to ensure the fine dispersion of particles without agglomeration and aging after some time or during experimentation.

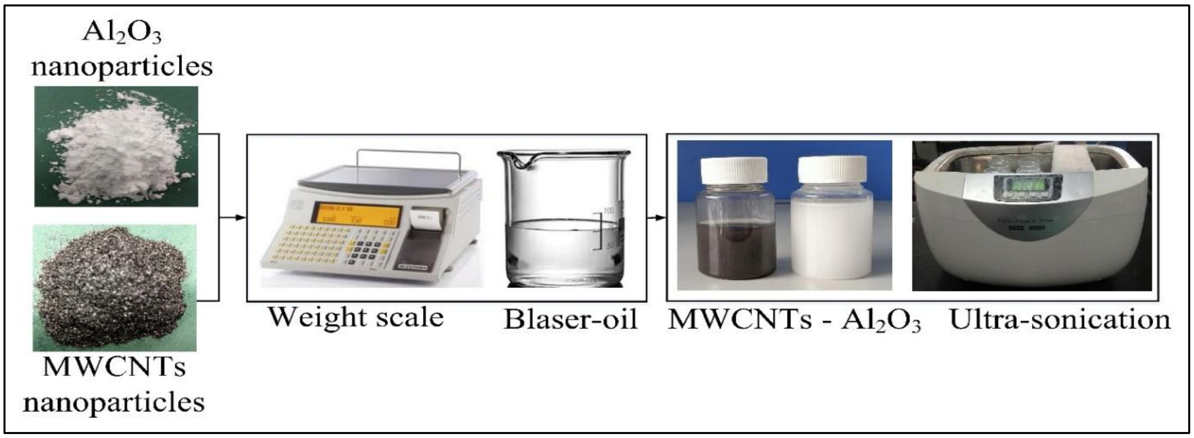

Figure 4: Two-step method to prepare hybrid nanofluids

The MQL system comprises a compressor, nanofluids reservoir, and an adjustable nozzle. MQL chamber mixes the oil and air to imping on the cutting zone. In MQL, an atomizing nozzle is fixed near the cutting zone to supply air-oil (containing hybrid nanofluids) mixture at the tool-chip interface. The two adjustable nozzles, 20 mm far from the tool-workpiece contact at an angle of 40^o from the workpiece surface.

2.3 Responses measurement

Cutting forces in milling are critical characteristics of a process that has a direct relation with the cutting tool, material hardness, and precision of the machine tool. The Kistler dynamometer was utilized to measure 3-dimensional forces such as cutting force, radial force, and feed force. This system amplifies the multi-channel signals, processes the data acquisitions, and displays the force signals (F_x=radial force, F_y=feed force, and F_z=normal force). The sampling frequency of data collection was set as 5000 Hz. In order to evaluate the effect of variables under cooling/lubrication in the milling process. Similarly, temperature elevation in machining is measured with a Fluke-Ti32 thermal infrared camera. The roughness of the outer surface of the workpiece is a standard indicator of the service life of the final product. The surface roughness was measured with the Surf-test (Mahr-1 Perthometer) for a 5.6 mm length of measurement. The workpiece material hardness is a factor that affects the reliability of the final product. The experimental details regarding the cooling system, measuring setup of machining characteristics are illustrated in a schematic Fig. 5.

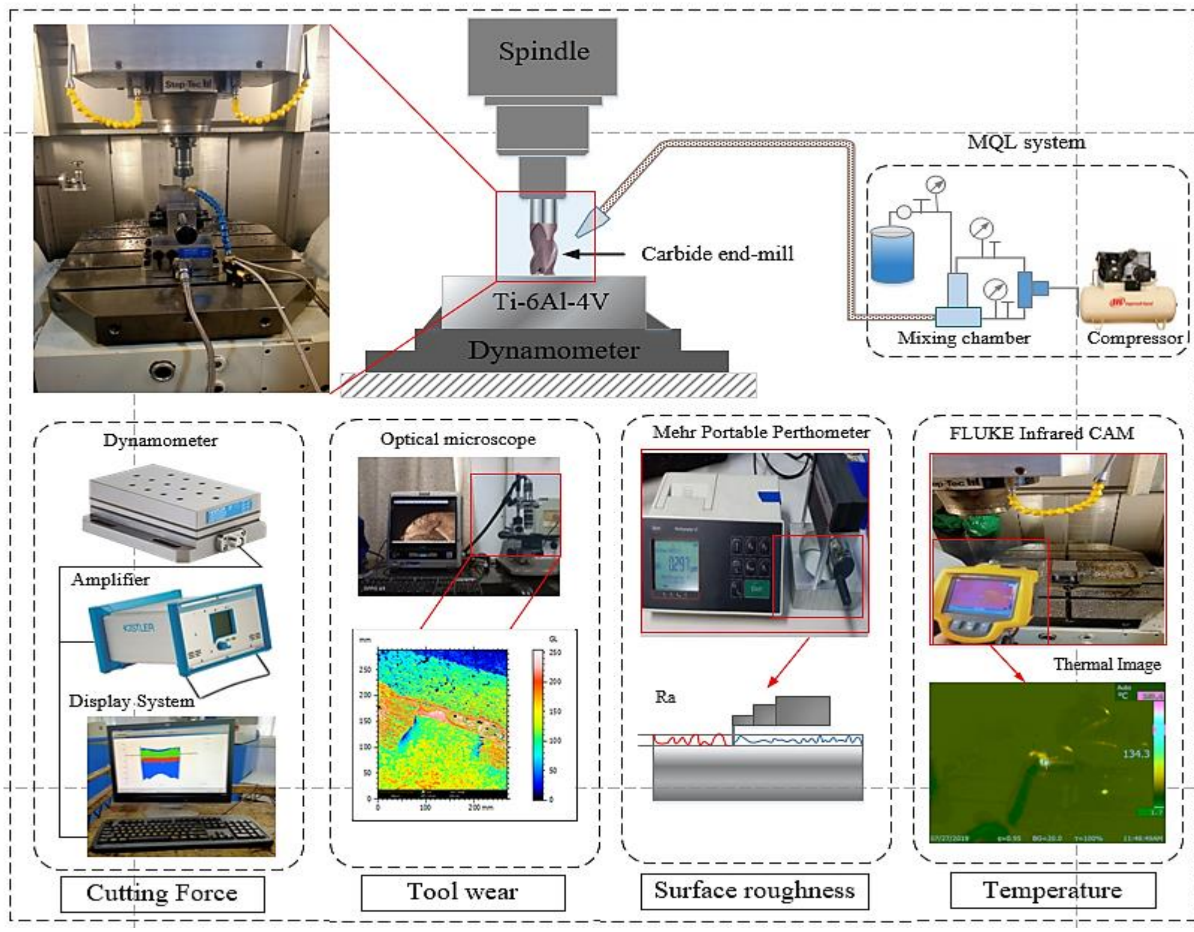

Figure 5: Minimum quantity lubrication system for automatic lubrication

3. Results and discussion

In this section, the experimental findings are collected and discussed in detail under different input variables. Based on Taguchi-method, milling characteristics such as cutting force, cutting temperature, and surface quality were evaluated under the effect of concentration, flow rate, and air pressure. According to Taguchi L_{16} orthogonal array, the experimental results have listed in Table. 3. Moreover, the S/N ratio was provided for each response value.

Table 3: Taguchi based experimental design and measured responses

Run #	Control parameters			Performance measures			Signal to noise ratios		
	Conc	fr	Ap	F_R (N)	T (ºC)	Ra (µm)	S/N_F_R	S/N_T	S/N_Ra
1	0.06	40	0.5	45.73	229.34	1.38	-33.20	-47.21	-2.80
2	0.06	80	0.6	42.12	208.43	1.21	-32.50	-46.38	-1.66
3	0.06	120	0.7	33.72	178.33	1.12	-30.56	-45.02	-0.98

4	0.06	160	0.8	34.15	168.21	0.97	-30.67	-44.52	0.26
5	0.12	40	0.6	45.4	218.68	1.26	-33.14	-46.80	-2.01
6	0.12	80	0.5	36	194.81	1.21	-31.13	-45.79	-1.66
7	0.12	120	0.8	36.51	162.91	0.92	-31.25	-44.24	0.72
8	0.12	160	0.7	27.8	159.33	0.98	-28.88	-44.05	0.18
9	0.18	40	0.7	39.45	214.35	1.18	-31.92	-46.62	-1.44
10	0.18	80	0.8	41.83	175.13	1.04	-32.43	-44.87	-0.34
11	0.18	120	0.5	25	163.83	1.05	-27.96	-44.29	-0.42
12	0.18	160	0.6	24.6	164.78	0.83	-27.82	-44.34	1.62
13	0.24	40	0.8	43.42	195.03	0.91	-32.76	-45.80	0.82
14	0.24	80	0.7	31.6	176.84	0.76	-29.99	-44.95	2.38
15	0.24	120	0.6	24.3	148.73	0.67	-27.71	-43.45	3.48
16	0.24	160	0.5	26	159.82	0.57	-28.30	-44.07	4.88

F_R =Resultant force, T=Cutting temperature, Ra=Surface roughness

The S/N ratio was calculated through 'less the better' formula using Minitab.18.1 software presented in Equ.1 and outputs were placed in Table 3. In addition, ANOVA for S/N ratio, having each performance measure, was determined to confirm the model significance as well as an individual variable contribution (Table 4).

Table 4: ANOVA of signal to noise based individual response

Performance measures		Conc	Fr	Ap	% Error	Total sum
F_R	Degree of Freedom	3	3	3	6	15
	Seq SS	10.684	39.257	6.977	1.971	58.89
	Adjusted MS	3.5613	13.08	2.3255	0.3285	-
	F-value	10.84	39.84	7.08		
	P-Value	0.008	0.000	0.021		
	% contribution	18.14%	66.65%	11.65%		
T	Seq SS	3.03	15.51	0.5235	0.4496	19.52
	Adjusted MS	1.01	5.17	0.174	0.07493	
	F-value	13.48	69.0	2.33		
	P-Value	0.004	0.000	0.174		
	% contribution	15.52%	79.39%	2.69%		
Ra	Seq SS	41.5364	21.1734	0.4779	2.4403	65.628
	Adjusted MS	13.8455	7.0578	0.1593	0.4067	
	F-value	34.04	17.35	0.39		
	P-Value	0	0.002	0.764		
	% contribution	63.31%	32.26%	0.73		

It is pertinent to mention that the p-value is less than 0.05, depicting that each parameter in the model has a significant contribution to the model. For total force F_R, coefficient of determination (R^2) is 96.65%, adjusted $R^{2,}$ and predicted R^2 are close to each other (difference <0.2). Similarly, for temperature T, R^2=97.7%, and surface roughness R^2=96.22%, respectively. The mean value of the S/N ratio for each parameter at different levels is exhibited in Table 5.

Table 5: The mean S/N ratio at each parameter levels

Performance measures	Levels	Input variables mean signal to noise (S/N) ratio		
		Conc%	Flow rate	air pressure
F_R	1	-31.73	-32.75	-30.15
	2	-31.10	-31.51	-30.29
	3	-30.03	-29.37	-30.34
	4	-29.69	-28.92	-31.77
T	1	-45.78	-46.61	-45.34
	2	-45.22	-45.50	-45.24
	3	-45.03	-44.25	-45.16
	4	-44.57	-44.24	-44.86
Ra	1	-1.29	-1.36	0.00
	2	-0.69	-0.32	0.36
	3	-0.15	0.70	0.03
	4	2.89	1.74	0.37

3.2 Effect of hybrid Al_2O_3-MWCNTs MQL on heat transfer

In the process of material removal, most of the heat generates at the primary and secondary shearing zone. The most of heat generated in the workpiece material is due to shear and rubbing, while in the tool material is due to friction, rubbing, and distribution of heat at rake and flank face. The quasi-steady-state heat model is normally used to define the heat distribution in the workpiece [21].

$$T_w = \frac{q}{\pi k_w} \int_0^L e^{-(\frac{V_{ft}\,(X-a)}{2\alpha}} K_0 \left\{ \frac{V_{ft}}{2\alpha} [(X-a)^2 + Z^2]^{0.5} \right\} f(a) da \qquad (1)$$

Where q is the frictional or shear heat, $f(a) = (1 + (2a/l_c))$, K_0 is the Bessel function, α is the thermal diffusivity of the workpiece, $L = underformed\ chip\ thickness/Sin\varphi$. Therefore, heat generation can be evaluated through this relation. In this place, it is assumed that total heat generation in the workpiece and the tool remains equal. The following relation depicts this assumption [22].

$$T_{M_{workpiece-shear}} + T_{M_{workpiece-rubbing}} + T_{workpiece-heatloss} = T_{M_{tool-rubbing}} + T_{M_{tool-friction}} + T_{M_{induced\,flank}} + T_{M_{induced\,rake}} - T_{tool-heatloss} \qquad (2)$$

As MQL is an air-oil mixture impinged on the tool-chip interface, it dissipates heat from the tool and workpiece. Due to oil-mixture, the heat losses in X, Y, and Z-directions can be defined as follows [22];

$$T_{hl} = \frac{q_{hl}}{2\pi k_t} \int_0^{Lc} \int_{-w/2}^{w/2} \left[\frac{1}{R_i} + \frac{1}{R_{i'}} \right] d_y d_x \qquad (3)$$

$R_i = \sqrt{(X-x)^2 + (Y-y)^2 + z^2}$; $R_i' = \sqrt{(X-(2L-x)^2 + (Y-y)^2 + z^2}$; and

$q_{hl} = h(T_{tool} - T_{fluid})$ h= heat transfer coefficient.

During the milling process, the temperature was measured with the Fluke infrared camera fixed at an appropriate distance from the tool-workpiece interface. Temperature measurement depicts the peak temperature for each milling pass. The measured temperature under dry and MQL hybrid nanofluids mist was displayed in Fig.6.

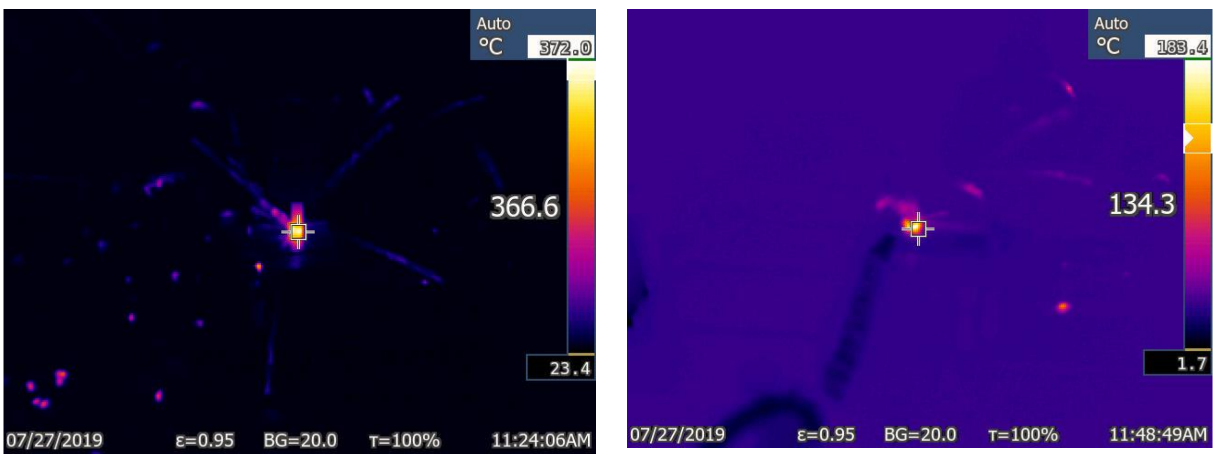

(a) (b)

Figure 6: Temperature under (a) dry and (b) MQL hybrid nanofluids

Accordingly, the maximum temperature under dry condition is 372 ºC, while under MQL hybrid nanofluids are 183 ºC. In addition, at different MQL parameters, the temperature was collected and plotted in Fig.7. Fig.7(a) demonstrates the S/N ratio of temperature at different levels of nanofluids concentration, Conc (wt%), flow rate, fr (mL/h), and air pressure, Ap (MPa). As the criteria defined for temperature are 'smaller the better,' that is why the flow rate has provided less S/N ratio of temperature at high and low levels of temperature. It is valuable to emphasize that the flow rate was the most significant parameter affecting temperature, followed by concentration and air pressure, respectively. This temperature reduction can be associated with the appropriate lubrication of hybrid nanoparticles that increased the cooling capacity, and efficiently dissipated heat from the cutting zone and controlled the cutting temperature. Due to the high

wettability of multiwalled nano additives, it formed a shielding layer of nanoparticles and reduced the friction. In addition, various sized nanoparticles having high heat-carrying capacity lowered the cutting temperature [23]. That is why a high flow rate of MQL has reduced the temperature efficiently. Fig.7(b) shows the 3D surface plot of temperature under simultaneous variation of concentration and flow rate. The temperature was decreased with the increase of the concentration and flow rate at all the levels of the parameters. It is worthy of mentioning that the lowest temperature was 148 ºC at the highest levels of the concentration and flow rate. The key reason behind the significant reduction of temperature is that high flow rate and concentration of nanofluids have extended capacity to absorb the tool-chip heat through Al_2O_3-MWCNTs particles. The high heat absorption of hybrid nano-additives also dissipates heat quickly from the cutting region to chip or fluid. As only MWCNTs have almost 150% higher thermal conductivity than the base fluid. So, MWCNTs show better performance regarding the heat transfer properties [24]. Fig.7(c) shows the simultaneous effect of concentration and air pressure on the milling temperature. The cutting temperature was decreased with increasing concentration and air pressure. The lowest temperature (152 ºC) was achieved at the highest levels of concentration and air pressure. The reduction in temperature can be attributed to the better morphology, and different sized nano-additives penetrated well at the cutting zone, dispersed in the base fluid due to weak Vander Waals forces and higher wettability has extracted heat well. Also, due to high pressure, the evaporation phenomenon to dissipate heat was prominent. This phenomenon had effectively prevented the elevation of temperature in the cutting zone. Fig.7(d) shows the 3D surface plot of temperature under the simultaneous effect of flow rate and air pressure. The temperature was reduced by increasing flow rate and air pressure. The higher flow rate added more nanofluids assisted fine mist at high air pressure. In the process of the fine penetration of hybrid nanofluids, the spherical and cylindrical shapes of nanoparticles having taken advantage to behave like spacers at the tool-chip interface to directly touch the tool to workpiece surface ultimately reducing the frictional heat generation. Considering advantages of vegetable oils, fine droplets of vegetable oil having a polar nature, align themselves on the surface of the workpiece, forming a thin lubrication film providing adequate lubrication compared to non-polar nature of cutting oils. Therefore, MQL with vegetable oil has reduced frictional temperature by applying hybrid lubri-cooling.

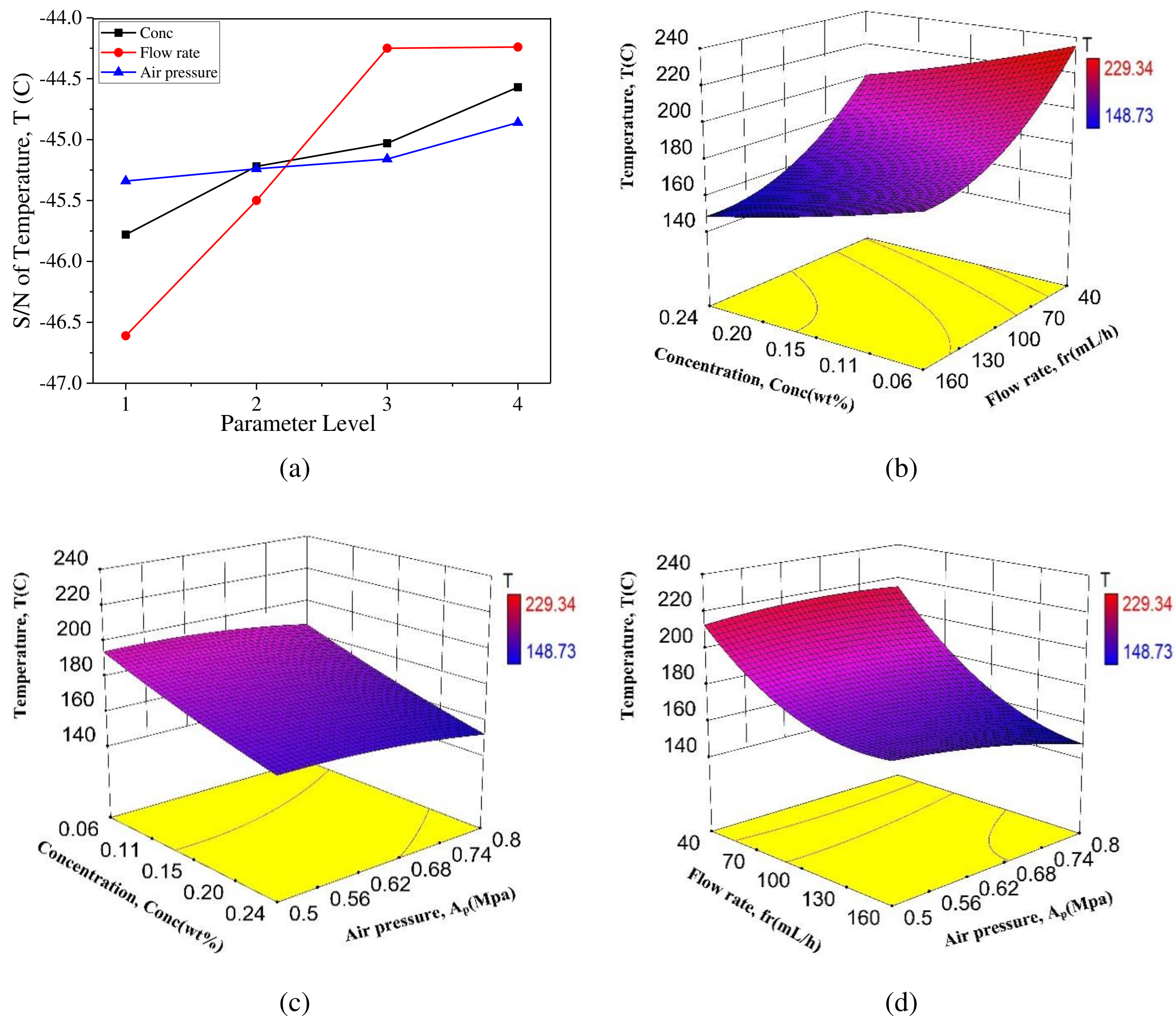

Figure 7: **(a)** S/N ratio of temperature T, 3D surface plot of **(b)** Conc (wt%) vs. f_r(mL/h) **(c)** Conc(wt%) vs. A_p (MPa) **(d)** f_r (mL/h) vs. A_p (MPa)

3.1 MQL parameters effect on resultant force

The cutting force is very useful in engineering for machine designs and machining settings, although the resultant average force is not the maximum value in the milling process [25]. As the end-mill contains several teeth to cut the material simultaneously, the average cutting force per teeth per cut in x, y, and z-direction (refer Fig.8) are:

$$F_{XT} = \sum_{i=1}^{z_c} \delta(\mathrm{i}).\, F_{xi}\ (\psi_i)$$

$$F_{YT} = \sum_{i=1}^{z_c} \delta(\text{i}).F_{yi}\ (\psi_i)$$

$$F_{ZT} = \sum_{i=1}^{z_c} \delta(\text{i}).F_{zi}\ (\psi_i) \quad (4)$$

While ψ_i is cutting angle, z_c =number of teeth cutting simultaneously (can't be rounded-off), and $z_c = \frac{z \times \psi_s}{360}$, z is number of teeth in end-mill, ψ_s is swept angle($\psi_s = \psi_2 - \psi_1$).

$\delta(\text{i}) = 1$ when $\psi_1 \leq \psi \leq \psi_2$, $\delta(\text{i}) = 0$ if *otherwise*

F_{XT} , F_{YT} and F_{ZT} are the average force per tooth in x, y, and z directions. The resultant force F_R was determined through the formula of total force F;

$$F_R = \sqrt{F_x^2 + F_y^2 + F_z^2} \quad (5)$$

Here F_x depicts the radial force component, F_y shows the feed force component, and F_z shows the normal force to the workpiece surface. The resultant milling force consists of elements induced due to the involved mechanism of the machining process.

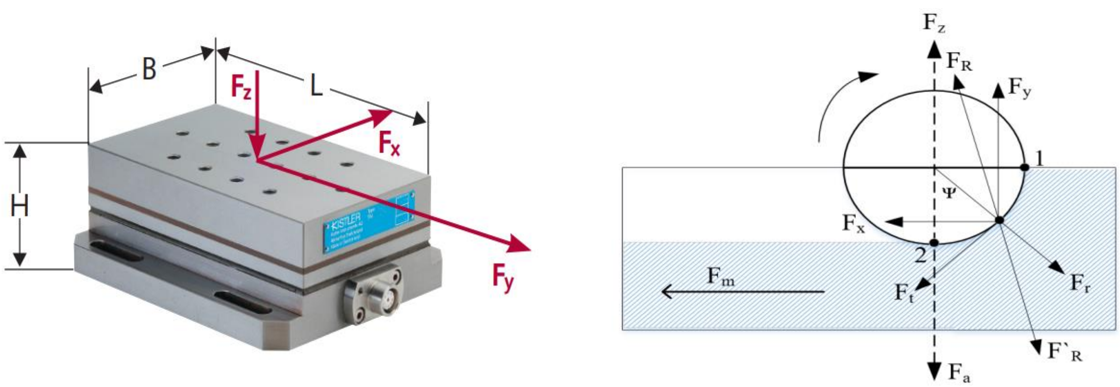

Figure: 8 (a) Force components Fx, Fy and Fz on a dynamometer (b) The force components in the milling process [25]

Fig.9(a) demonstrates the S/N ratio of the resultant force under variation of concentration, Con (wt%), flow rate, fr (mL/h), and air pressure, Ap (MPa). It can be seen from Fig.9a that the S/N ratio of resultant force F_R(N) is smaller at the low levels of concentration and flow rate, and it increases by increasing the concentration and flow rate. However, the S/N-ratio of F_R is higher at low levels of air pressure and decreases at the highest level of the air pressure. As the S/N ratio of F_R is smaller, the better, so by increasing the concentration and flow rate, the resultant force F_R was decreased. While increasing air pressure, the resultant force F_R was slightly increased; however, the effect of air pressure was not so high on the effect

of the resultant force. Fig.9(b) depicts the 3D response surface plot of underscoring the simultaneous effect of concentration and flow rate on resultant force F_R. The resultant force F_R decreased with the increase of concentration and flow rate. However, the effect of flow rate on the reduction of resultant force F_R was significantly higher than in concentration.

The highest resulting force F_R was 24N at the highest level of concentration and flow rate. The effectiveness of nanofluids concentration and flow rate towards the reduction of resulting force F_R can be associated with the addition of hybrid nanoparticles provided lubrication due to a ball-bearing effect at the cutting zone. The suspended hybrid nano-additives of spherical and cylindrical shapes in Blaser oil form a thin layer of lubrication that reduces friction between the tool-chip interface. The high flow rate has more ability to prevent direct contact of end-mill with the workpiece surface from lowering down the cutting forces [26]. Fig.9(c) shows the simultaneous effect of concentration and air pressure on the resulting force F_R. The resulting force F_R was decreased with the increase of concentration and slightly increased with the increase of the air pressure. The lowest resulting force F_R of 25 N was achieved at a high level of concentration and the lowest level of air pressure. It is important to mention that a slight increase in F_R was due to the nozzle angle (about 65^o) that directly put air pressure on the tool-chip interface and compressed the workpiece below. That may be one of the possible reasons behind a slight increase in the resulting force. Fig.9(d) underscores the 3D response surface plot of flow rate and air pressure. The resulting force F_R is decreased with the increase of flow rate and increased with the increasing air pressure. The high flow rate of MQL fine mist contains a high proportion of nano-additives suspended in Blaser oil behaves as a polar nature coolant. The molecules of oil align themselves in opposite charge poles. These strong polar bonds and suspended nanoparticles reduce friction significantly. In addition, the higher wettability and viscosity allow the fine mist to stay longer on the workpiece and tool surfaces. The nano-additives penetrate well into the tool-chip interface. The MWCNTs have layered structures of carbon behaves as a lubricant, while the spherical shape of the Al_2O_3 nano-additives shows a rolling effect reducing the friction and cutting forces.

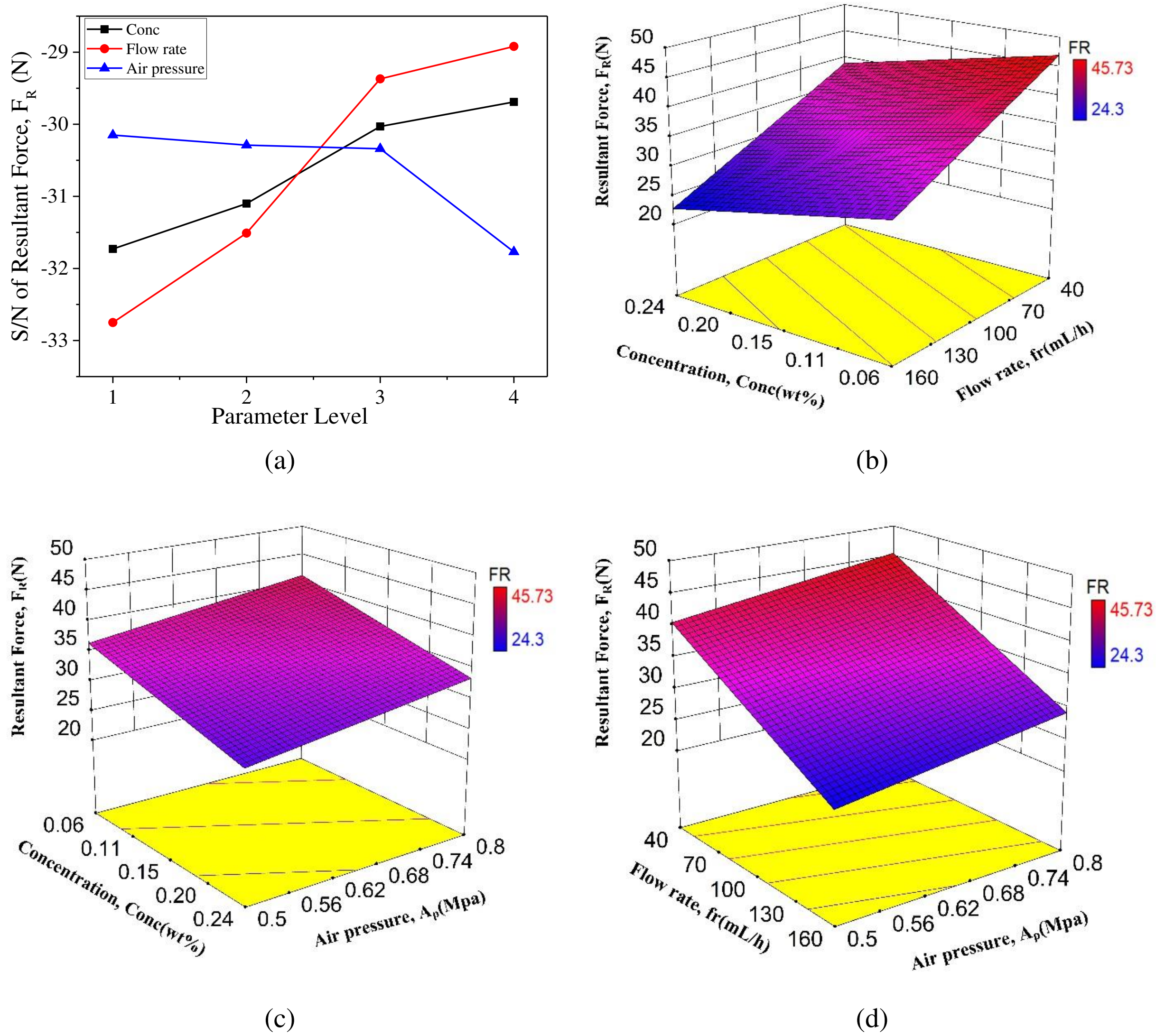

Figure 9: **(a)** S/N ratio of resultant force F_R, 3D surface plot of **(b)** Conc(wt%) vs. f_r(mL/h) **(c)** Conc(wt%) vs. A_p (MPa) **(d)** f_r(mL/h) vs. A_p (MPa)

3.4 MQL parameters effect on surface roughness

The arithmetic average height parameter (R_a), also named CLA (center-line average), is the most frequently used roughness parameter for quality control. For a specific length of the sample, the average irregularities/deviations from the mean line are named as an average surface roughness (R_a). The l_r is the measurement length, l_n is the necessary length for measurement, $h_i \ldots\ldots h_n$ are the absolute distance of each point from the mean line. The equation for the arithmetic-mean height can be defined as follows:

$$R_a = \frac{1}{l}\int_0^l |h(x)|\,.\,dx \qquad (6)$$

R_a=average height(μm); *l*=number of intersections of the profile.

Fig.10(a) shows the surface plots of the S/N ratio of surface roughness corresponding to the simultaneous effect of concentration, flow rate, and air pressure. The S/N ratio of surface roughness increased with the increase of concentration, flow rate, and air pressure; however, the concentration of nanofluids affected the S/N ratio of surface roughness considerably at the high level. Fig.10(b) illustrates the 3D response of the concentration and flow rate on the surface roughness. The surface roughness decreases with the increase of the concentration and flow rate; however, the surface roughness is more sensitive to concentration than the flow rate. The minimum surface roughness with 0.57μm was achieved at the maximum level of concentration and flow rate. The significant effect of the nanofluids of concentration on the surface roughness can be referred to as the tribological properties of MWCNTs. Although there are no research findings regarding the tribological superiority of MWCNTs than Al_2O_3; it is claimed that MWCNTs are better lubricants than Al_2O_3. As the MWCNTs are carbon particles, superior surface area and their structure can sustain high pressure and fill the micro-spaces on the workpiece surface. In this way, the surface finish was improved under the high concentration of hybrid nanofluids. Fig.10(c) shows the simultaneous effect of concentration and air pressure on surface roughness. It is identified that surface roughness was decreased with increasing concentration and air pressure; however, surface roughness was more dependent on concentration than the air pressure. The minimum surface roughness as 0.64 μm was achieved at the highest level of concentration and air pressure. Fig.10(d) underscores the effect of flow rate and air pressure on the surface roughness. The surface roughness was decreased with the increase of flow rate and air pressure. This phenomenon can be associated with the cooling/lubrication characteristics of the hybrid nanofluids, extended the wettability, stayed longer on the tool cutting edge, dissipated heat, and provided lubrication as discussed by the earlier studies [10]. This mist can penetrate and form a tribo-film on the surface of the tool and the workpiece and decrease the coefficient of friction. Accordingly, the hybrid nanofluids under high flow rates behave like rolling, polishing, and filming actions to fill the empty spaces on the workpiece surface. That is why hybrid nanofluids having spherical shaped Al_2O_3 and cylindrical MWCNTs in different sizes provide the synergistic on workpiece surface than single nanofluids assisted as reported by Ref. [27].

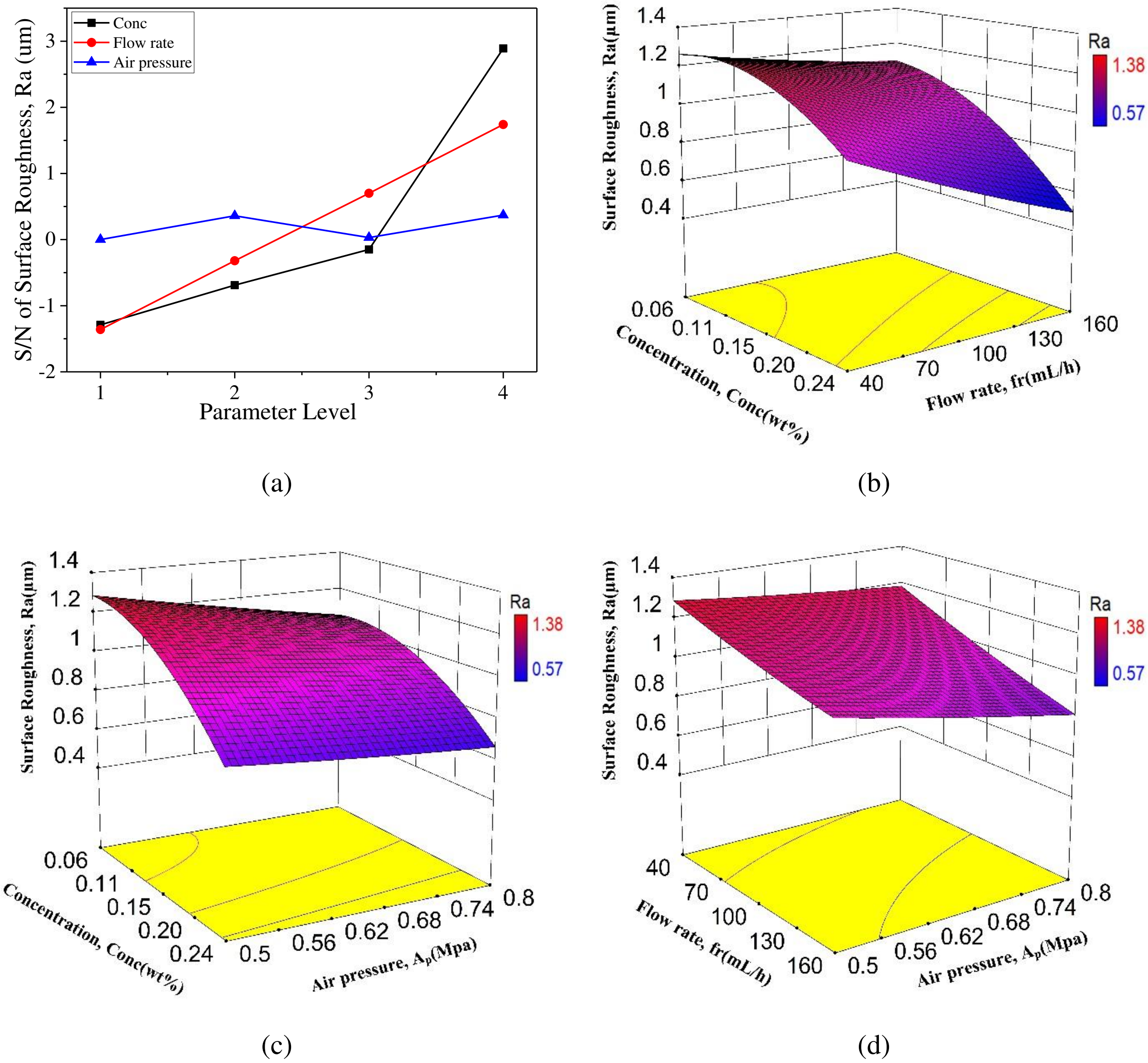

Figure 10: **(a)** S/N ratio of temperature Ra, 3D surface plot of **(b)** Conc (wt%) vs. f_r (mL/h) **(c)** Conc (wt%) vs. A_p (MPa) **(d)** f_r (mL/h) vs. A_p (MPa)

3.5 Tool wear mechanism

The cutting forces and temperature are mostly influenced by the wear of the cutting tool. The wear of cutting tools depends upon tool materials, type of coatings, cutting conditions, and cooling/lubrication. In this section, the effect of nanofluids assisted MQL associated parameters (concentration, flow rate, air pressure) were studied to explore the effect of hybrid nanofluids MQL on tool wear behavior. The % concentration, flow rate, and air pressure are fixed as 0.24 wt%, 120 mL/h, and 0.6 MPa, respectively. The state of the cutting tool was highlighted through the scanning electron microscopy (Fig.11). The dominant wear patterns under MQL are the abrasive wear, coating peeling, and chip adhesion. From Fig. 11, it can

be determined that less severe abrasive wear was observed between the cutting tool and the workpiece. Besides, coating peeling was appeared due to chip sliding on the tool surface and formation of saw tooth chips and BUE during cutting. Ezugwu et al. [28] have reported BUE formation on the cutting tool in the machining of hard-to-cut materials is one of the issues encountered during cutting. It can be said that when the cutting temperature reaches a critical stage, the tendency of chip welding becomes high enough owing to the chemical closeness between workpiece material and cutting tool material.

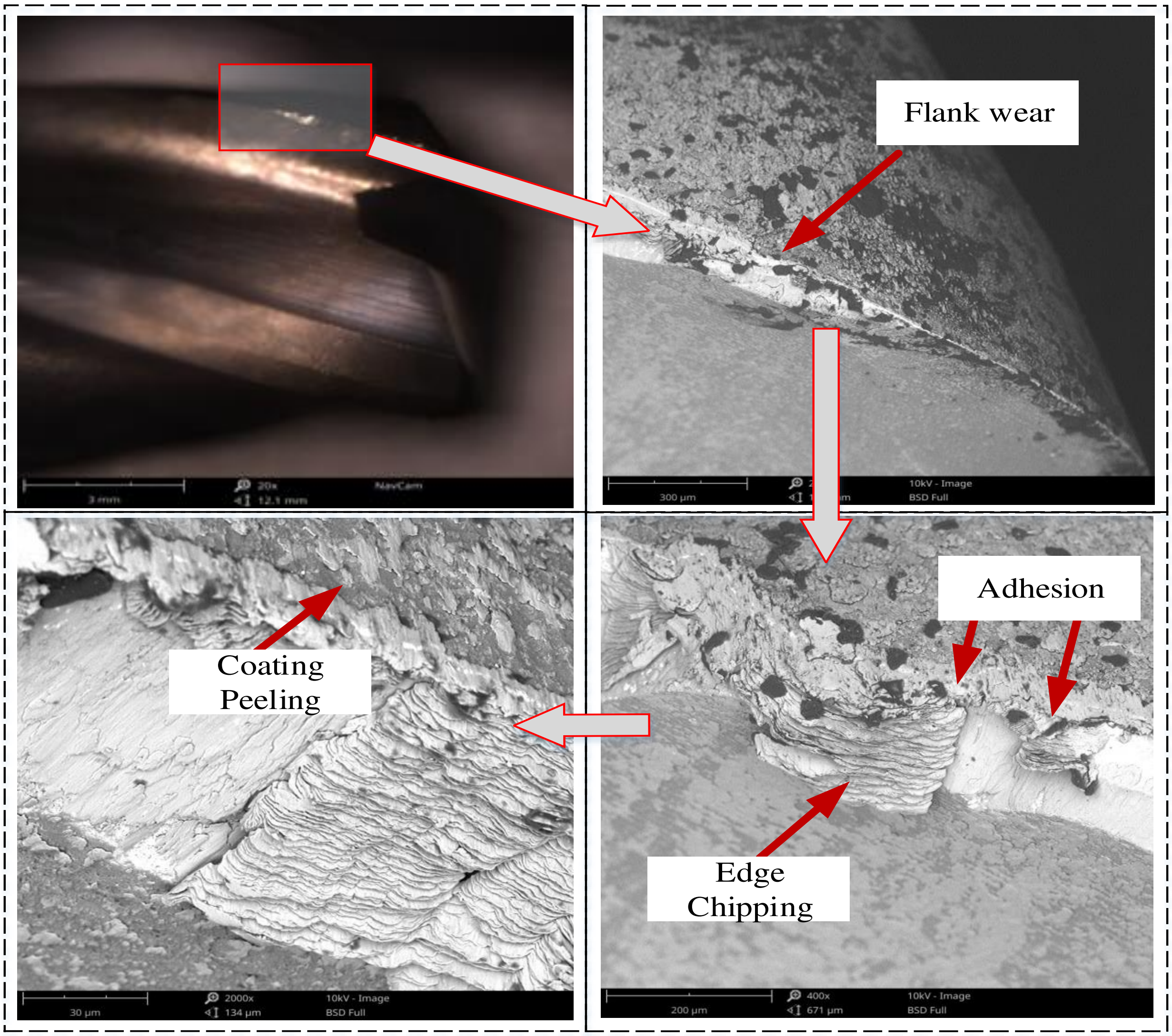

Figure 11: The SEM analysis of the milling tool under 0.24 wt% concentration, 120 mL/h flow rate, and 0.6 MPa air pressure

As the cutting tool starts cutting, due to poor thermal conductivity of Ti-6Al-4V, cutting tool scratches leading to thermal cracks initiation on the cutting edge due to imbalanced heat and fatigue on different portions of the cutting tool. As the cutting tool continues to cut, thermal crack energy starts accumulating.

When the thermal crack energy exceeds the crack propagation threshold, enabling thermal cracks initiation. As a result, this phenomenon lowers the coating thickness, reduces its strength, and accelerates coating peeling [29]. The mist carrying hybrid nano-additives penetrated well at the tool-chip interface due to air pressure, formed a tribo-film. It significantly reduced the severe edge chipping, coefficient of friction, and adhesion from the tool cutting edge. These advances with superior lubrication/cooling allowed chip adhesion and coating peeling to occur in a smaller area of the cutting edge. The reduction of such sever chipping may occur due to nano-additives behaving as spacers between tool-workpiece interface and prevented direct tool contact, helped to slip the chip on the cutting edge rather than adhesion.

3.6 Surface topography and chip morphology

The surface topography of the machined workpiece is highlighted in Fig.12. It is obvious that MQL conditions have generated smooth, with fewer peaks and valleys. It can be attributed to the smooth wear of the cutting tool and less chip adhesion and welding under hybrid nanofluid conditions. The feed marks were appeared on the surface owing to the interaction of the current tool path with the neighboring tool paths. Thus, the feed marks were blurred, and an increase in feed marks with increasing the workpiece length. However, very fewer chips sticking on the newly generated surface were observed because of the pressured mist has flown away from the chips.

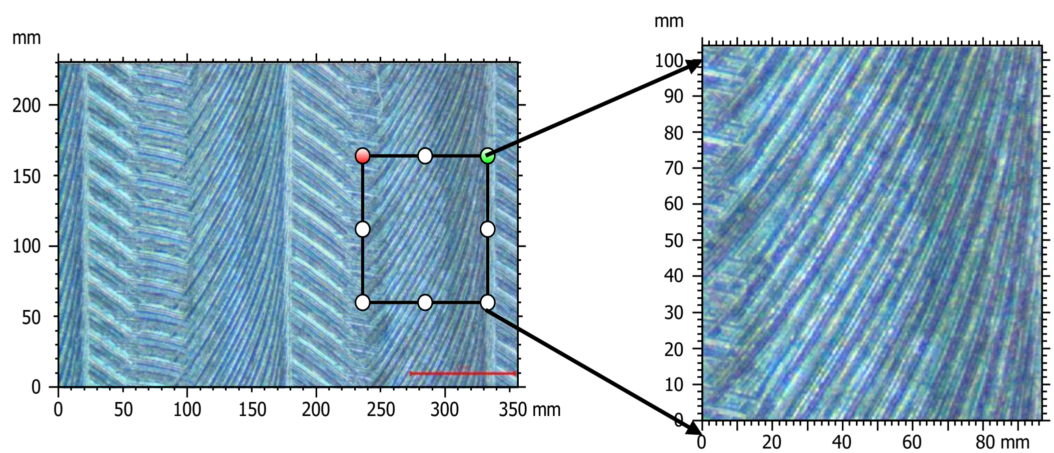

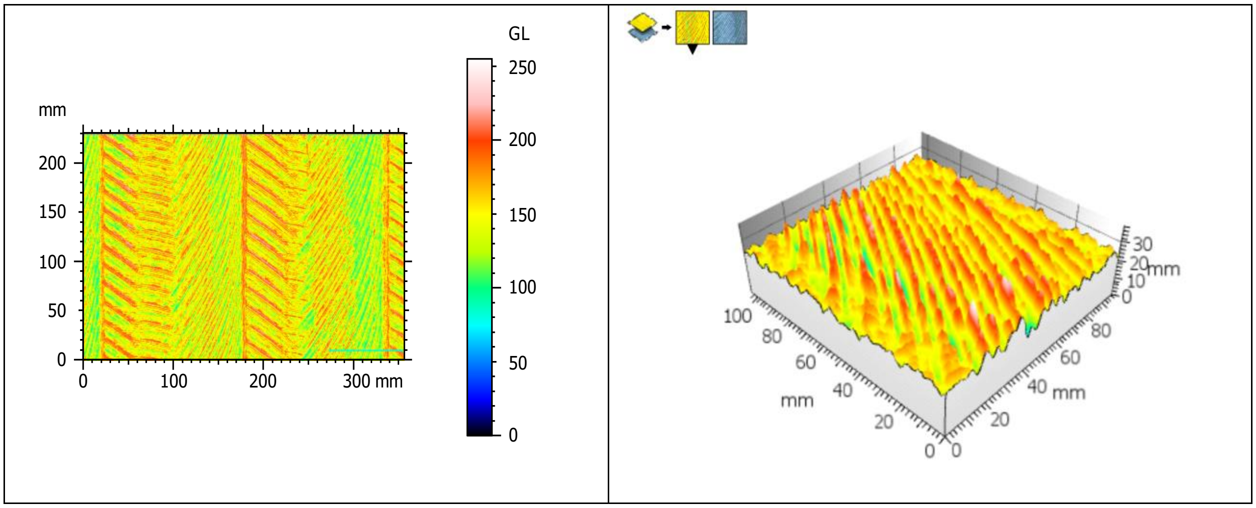

Figure 12: Surface topography of the machined surface at nanofluids concentration of 0.24vol%, 120ml/h of flow rate at 0.6MPa of air pressure

Chip morphology analysis is presented to relate the surface quality and material behavior under machining. Although a different type of chips produces in the machining of different materials, however, cooling/lubrication methods also have a significant effect on the shape of chips. For example, machining of Ti-6Al-4V provides discontinuous and saw-tooth chips. The chip analysis defines the tool-chip contact length, friction at the common interface, ultimately the heat generation at the secondary shearing zone. This heat generation and friction have a key role in the final shape of chip formation. The chip consisted of localized shear bands, form by phase change (dynamic recrystallization) due to exceeding thermal softening from strain hardening. The application of MQL also produces a varying chip morphology rather than varying chip thickness and serration distances. Fig.13 depicts the sawtooth and discontinuous chips at a closer view of chips having adiabatic shear bands. However, the backside of the chip underscored feed marks of shearing material in the feed direction of the cutting tool. The less severe feed marks (friction tracks) indicated the tribo-film formation and rolling effects of under hybrid nanofluids restricted these marks.

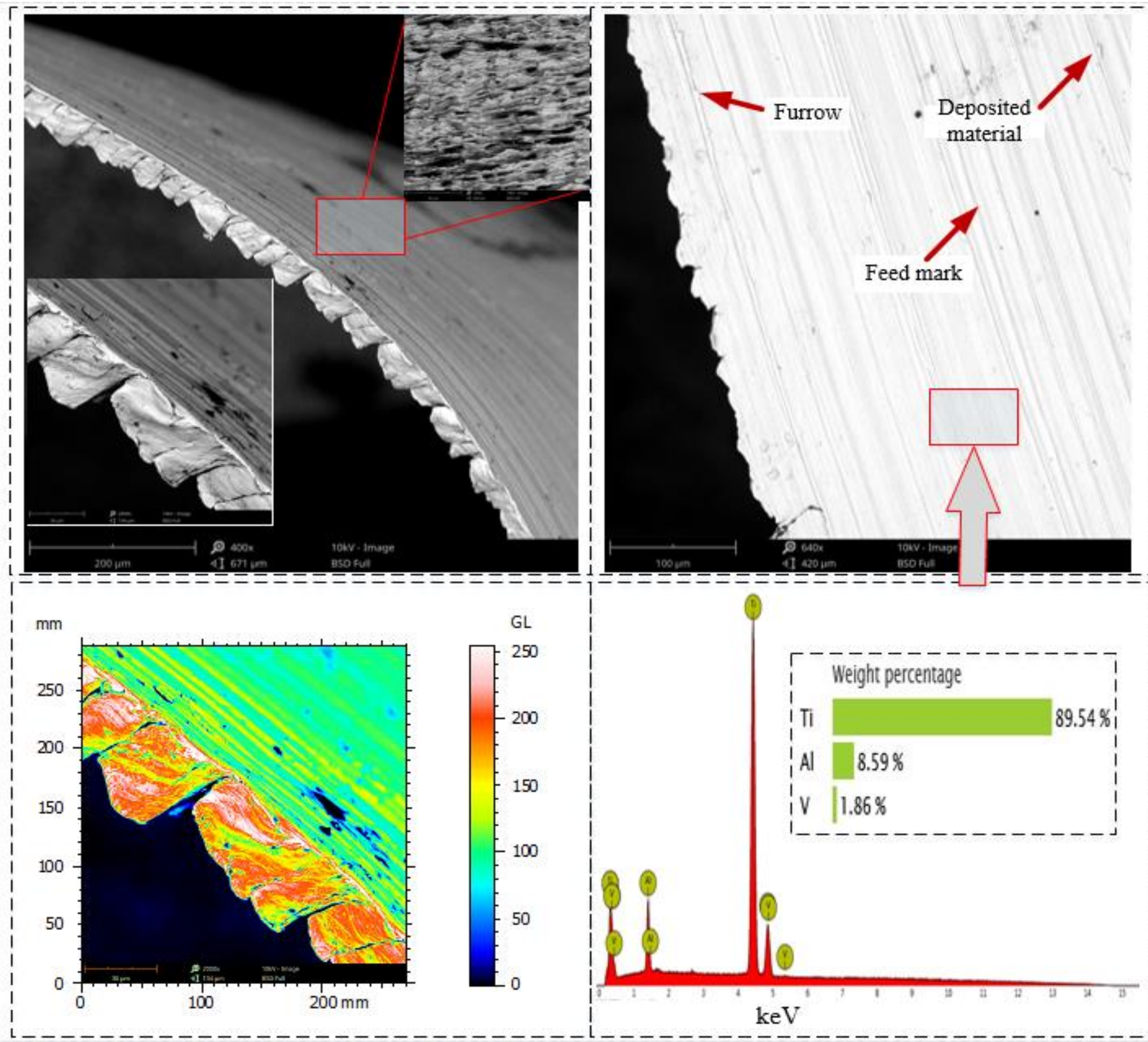

Figure 13: The SEM analysis of chip and EDS of the chip produced under MQL machining at a nanofluids concentration of 0.24vol%, 120ml/h of flow rate at 0.6MPa of air pressure

The energy-dispersive X-ray spectroscopy (EDS) analysis has underscored Ti, V, and Al components of chip analysis. To prevent the heat or transfer heat from the tool-chip interface, hybrid nanofluids MQL is expected to dissipate heat from the cutting region. In this way, it limits the thermal softening of the workpiece material and eases in chip flow by the presence of nano-additives at the tool-chip interface. In addition, the pressured nano-mist dissipated the generated heat and prevented chip welding which facilitates the chip flow, and that is owing to the presence of MWCNTs nano-additives. Also, due to the uniform strain on the material during cutting (i.e., low and high strain leads to the formation of saw-tooth chips), wider and lower in depth saw-tooth were observed under MWCNTs assisted MQL.

3.7 Tribology mechanism of hybrid (Al_2O_3-MWCNTs) nanoadditives

Several researchers have reported the superior thermal, physical, and rheological properties of hybrid nanofluids than single nanofluids in turning, milling, drilling, and metal forming [14,30]. The improved cutting conditions for the machining of difficult-to-cut materials are attributed to the hybrid nanofluids owing to thermal conductivity, lubrication to limit the heat and wear of the cutting tool. The variables sizes and shapes of the nanoparticles suspended in base fluid provide significant advantages during the cutting process. Also, understanding the possible mechanisms is highly essential (Fig.14).

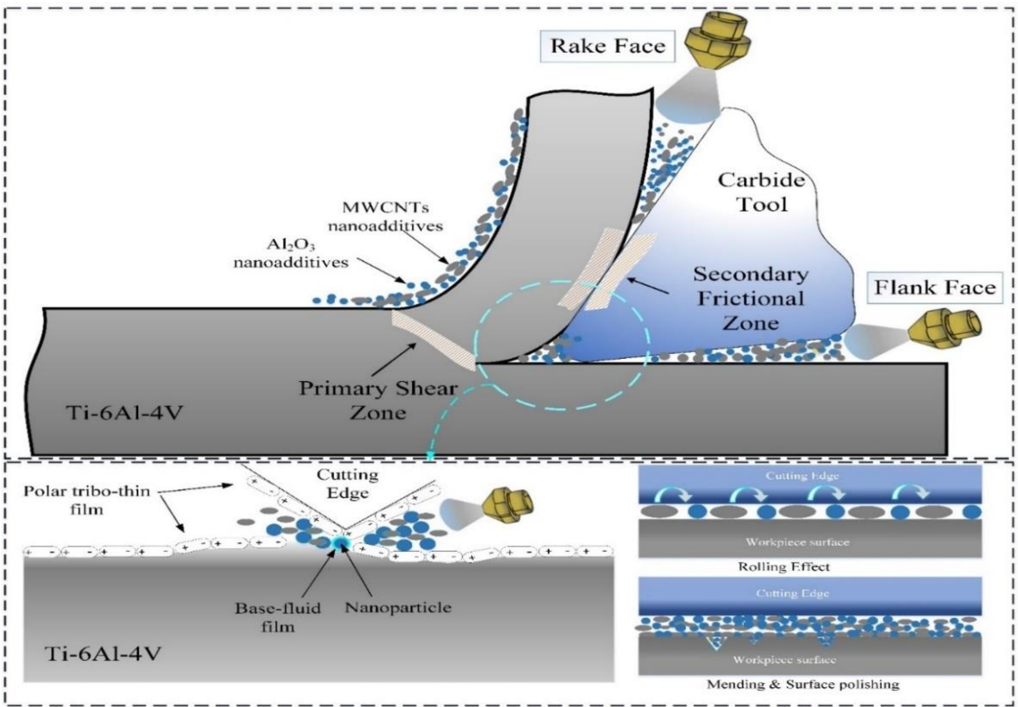

Figure 14: The hybrid nanofluids mechanism and effect on machining Ti-6Al-4V

The possible mechanisms of hybrid nanofluids are summarized as follows:

- A very fine mist emits from MQL nozzle as compressed air is mixed with hybrid nanofluids suspended fluids in 60:40 in a mixing chamber.
- The fine mist droplet carries nanoparticles surrounded by thin oil-film. This high-velocity mist penetrates well since it impinges and fills the tool pores and groves.
- Thus, mist droplets spread and form a dipolar thin film on the tool, and the workpiece surface enhances tribological characteristics and lowers the friction. Also, superior thermal conductivity and lubrication function of Al_2O_3-MWCNTs dissipates heat from the cutting zone.

- Increasing concentration of hybrid nanoadditives increased nanoparticles at the tool-chip interface, behave as spacers, and ball-bearing to limit the tool contact as well as chip contact length.
- Variables sizes and shapes of hybrid nanoadditives have advantages to fill the wide/close contact between the tool-workpiece. Also, fills micro-voids on workpiece surface due to external pressure, results in improving the workpieces surface roughness.

4. Conclusion and Future Work

In this research, the milling characteristics of Ti-6Al-4V under hybrid nanofluids assisted MQL conditions are investigated experimentally. The influence of Al_2O_3-MWCNTs on the milling force, temperature, and surface roughness are analyzed. The following conclusions are drawn:

1. When hybrid nanofluids are applied to the milling, it is observed the flow rate was the most significant parameter influenced resultant force, followed by concentration and flow rate. It could be associated with the tribo-film formation due to the high concentration of nanofluids showed excellent lubrication, regarding load-carrying, wear resistance at 0.24 wt%, and 160 mL/hr.
2. Regarding the cutting temperature, hybrid nanofluids assisted MQL reduced the shearing as well as frictional heat generation. The MQL flow rate played a significant role in the reduction of cutting temperature, followed by concentration and air-pressure. The hybrid nanofluids prevented the direct contact of the cutting tool with the workpiece to control the heat generation.
3. In respect of surface roughness, a significant improvement in surface quality was observed due to a reduction in chip adhesion, severe BUE formations, and a smooth machined surface. A considerable reduction in surface roughness was noticed under the increase of nano-additives concentrations, followed by flow rate and air pressure. It can be associated with the capability of different shape hybrid nanofluids behaved as ball-bearings and able to fill the micro-voids on the surface.

   The SEM analysis of tool flank-wear depicted less sever tool edge damage, chip-welding, and coating peeling. It principally can be attributed to the excellent penetration of nanofluids and forming a protective layer on the tool surface to slide the chip. Also, chip analysis depicts the clean back surface and less melting of saw-tooth chip edges. The surface topography confirms the less micro-adhesion of chips and material debris.

Conflict of Interest:

It is declared that authors have no conflict of interest

Acknowledgment and funding

The authors would also like to acknowledge the efforts made by Prof. Hitoshi Ohmori of Saitama University (Japan) for his valuable suggestions to improve the manuscript. The work is funded by the National Key Research and Development Project (2018YFB2002205).

References

[1] Mia M, Gupta MK, Lozano JA, Carou D, Pimenov DY, Królczyk G, et al. Multi-objective optimization and life cycle assessment of eco-friendly cryogenic N2 assisted turning of Ti-6Al-4V. Journal of Cleaner Production 2019;210:121–33. doi:10.1016/j.jclepro.2018.10.334.

[2] Paul S, Singh AK, Ghosh A. Grinding of Ti-6Al-4V Under Small Quantity Cooling Lubrication Environment Using Alumina and MWCNT Nanofluids. Materials and Manufacturing Processes 2017. doi:10.1080/10426914.2016.1257797.

[3] Jamil M, Khan AM, He N, Li L, Iqbal A, Mia M. Evaluation of machinability and economic performance in cryogenic-assisted hard turning of α-β titanium: a step towards sustainable manufacturing. Machining Science and Technology 2019:1–25. doi:10.1080/10910344.2019.1652312.

[4] Darshan C, Jain S, Dogra M, Gupta MK, Mia M. Machinability improvement in Inconel-718 by enhanced tribological and thermal environment using textured tool. Journal of Thermal Analysis and Calorimetry 2019. doi:10.1007/s10973-019-08121-y.

[5] Carvalho DOA, da Silva LRR, Sopchenski L, Jackson MJ, Machado ÁR. Performance evaluation of vegetable-based cutting fluids in turning of AISI 1050 steel. International Journal of Advanced Manufacturing Technology 2019. doi:10.1007/s00170-019-03636-y.

[6] Khan AM, Jamil M, Ul Haq A, Hussain S, Meng L, He N. Sustainable machining. Modeling and optimization of temperature and surface roughness in the milling of AISI D2 steel. Industrial Lubrication and Tribology 2018;71:267–77. doi:10.1108/ILT-11-2017-0322.

[7] Yıldırım ÇV, Kıvak T, Sarıkaya M, Erzincanlı F. Determination of MQL Parameters Contributing to Sustainable Machining in the Milling of Nickel-Base Superalloy Waspaloy. Arabian Journal for Science and Engineering 2017. doi:10.1007/s13369-017-2594-z.

[8] Ibrahim AMM, Li W, Xiao H, Zeng Z, Ren Y, Alsoufi MS. Energy conservation and environmental sustainability during grinding operation of Ti–6Al–4V alloys via eco-friendly oil/graphene nano additive and Minimum quantity lubrication. Tribology International

2020;150:106387. doi:10.1016/j.triboint.2020.106387.

[9] Saidur R, Leong KY, Mohammad HA. A review on applications and challenges of nanofluids. Renewable and Sustainable Energy Reviews 2011. doi:10.1016/j.rser.2010.11.035.

[10] Sidik NAC, Samion S, Ghaderian J, Yazid MNAWM. Recent progress on the application of nanofluids in minimum quantity lubrication machining: A review. International Journal of Heat and Mass Transfer 2017. doi:10.1016/j.ijheatmasstransfer.2016.11.105.

[11] Hegab H, Kishawy HA, Gadallah MH, Umer U, Deiab I. On machining of Ti-6Al-4V using multi-walled carbon nanotubes-based nano-fluid under minimum quantity lubrication. The International Journal of Advanced Manufacturing Technology 2018;97:1593–603. doi:10.1007/s00170-018-2028-4.

[12] Behera BC, Alemayehu H, Ghosh S, Rao PV. A comparative study of recent lubri-coolant strategies for turning of Ni-based superalloy. Journal of Manufacturing Processes 2017;30:541–52. doi:10.1016/j.jmapro.2017.10.027.

[13] Ahammed N, Asirvatham LG, Wongwises S. Entropy generation analysis of graphene–alumina hybrid nanofluid in multiport minichannel heat exchanger coupled with thermoelectric cooler. International Journal of Heat and Mass Transfer 2016. doi:10.1016/j.ijheatmasstransfer.2016.07.070.

[14] Jamil M, Khan AM, Hegab H, Gong L, Mia M, Gupta MK, et al. Effects of hybrid Al2O3-CNT nanofluids and cryogenic cooling on machining of Ti–6Al–4V. The International Journal of Advanced Manufacturing Technology 2019. doi:10.1007/s00170-019-03485-9.

[15] Nine MJ, Batmunkh M, Kim JH, Chung HS, Jeong HM. Investigation of Al 2O 3-MWCNTs hybrid dispersion in water and their thermal characterization. Journal of Nanoscience and Nanotechnology 2012. doi:10.1166/jnn.2012.6193.

[16] Zhang Y, Li C, Jia D, Li B, Wang Y, Yang M, et al. Experimental study on the effect of nanoparticle concentration on the lubricating property of nanofluids for MQL grinding of Ni-based alloy. Journal of Materials Processing Technology 2016;232:100–15. doi:10.1016/j.jmatprotec.2016.01.031.

[17] Hegab H, Umer U, Deiab I, Kishawy H. Performance evaluation of Ti–6Al–4V machining using nano-cutting fluids under minimum quantity lubrication. The International Journal of Advanced Manufacturing Technology 2018;95:4229–41. doi:10.1007/s00170-017-1527-z.

[18] Sharma AK, Katiyar JK, Bhaumik S, Roy S. Influence of alumina/MWCNT hybrid nanoparticle additives on tribological properties of lubricants in turning operations. Friction 2018. doi:10.1007/s40544-018-0199-5.

[19] Kumar Sharma A, Kumar Tiwari A, Rai Dixit A, Kumar Singh R. Measurement of Machining Forces and Surface Roughness in Turning of AISI 304 steel using Alumina-MWCNT Hybrid Nanoparticles Enriched Cutting Fluid. Measurement 2019:107078. doi:10.1016/j.measurement.2019.107078.

[20] Mia M, Dhar NR. Influence of single and dual cryogenic jets on machinability characteristics in turning of Ti-6Al-4V. Proceedings of the Institution of Mechanical Engineers, Part B: Journal of Engineering Manufacture 2017. doi:10.1177/0954405417737581.

[21] Hadad MJ, Tawakoli T, Sadeghi MH, Sadeghi B. Temperature and energy partition in minimum quantity lubrication-MQL grinding process. International Journal of Machine Tools and Manufacture 2012. doi:10.1016/j.ijmachtools.2011.11.010.

[22] Li KM, Liang SY. Modeling of cutting temperature in near dry machining. Journal of Manufacturing Science and Engineering, Transactions of the ASME 2006. doi:10.1115/1.2162907.

[23] Mia M, Morshed MS, Kharshiduzzaman M, Razi MH, Mostafa MR, Rahman SMS, et al. Prediction and optimization of surface roughness in minimum quantity coolant lubrication applied turning of high hardness steel. Measurement: Journal of the International Measurement Confederation 2018. doi:10.1016/j.measurement.2018.01.012.

[24] Li B, Li C, Zhang Y, Wang Y, Jia D, Yang M, et al. Heat transfer performance of MQL grinding with different nanofluids for Ni-based alloys using vegetable oil. Journal of Cleaner Production 2017. doi:10.1016/j.jclepro.2017.03.213.

[25] Alauddin M, El Baradie MA, Hashmi MSJ. Modelling of cutting force in end milling Inconel 718. Journal of Materials Processing Technology 1996. doi:10.1016/0924-0136(95)02113-2.

[26] Nam JS, Lee PH, Lee SW. Experimental characterization of micro-drilling process using nanofluid minimum quantity lubrication. International Journal of Machine Tools and Manufacture 2011. doi:10.1016/j.ijmachtools.2011.04.005.

[27] Sharma AK, Tiwari AK, Dixit AR. Prediction of temperature distribution over cutting tool with alumina-MWCNT hybrid nanofluid using computational fluid dynamics (CFD) analysis. The

International Journal of Advanced Manufacturing Technology 2018;97:427–39. doi:10.1007/s00170-018-1946-5.

[28] Ezugwu EO, Wang ZM. Titanium alloys and their machinability - A review. Journal of Materials Processing Technology 1997;68:262–74. doi:10.1016/S0924-0136(96)00030-1.

[29] Jamil M, Khan AM, Gupta MK, Mia M, He N, Li L, et al. Influence of CO2-snow and subzero MQL on thermal aspects in the machining of Ti-6Al-4V. Applied Thermal Engineering 2020;177:115480. doi:https://doi.org/10.1016/j.applthermaleng.2020.115480.

[30] Yıldırım ÇV. Experimental comparison of the performance of nanofluids, cryogenic and hybrid cooling in turning of Inconel 625. Tribology International 2019. doi:10.1016/j.triboint.2019.05.014.

Figures

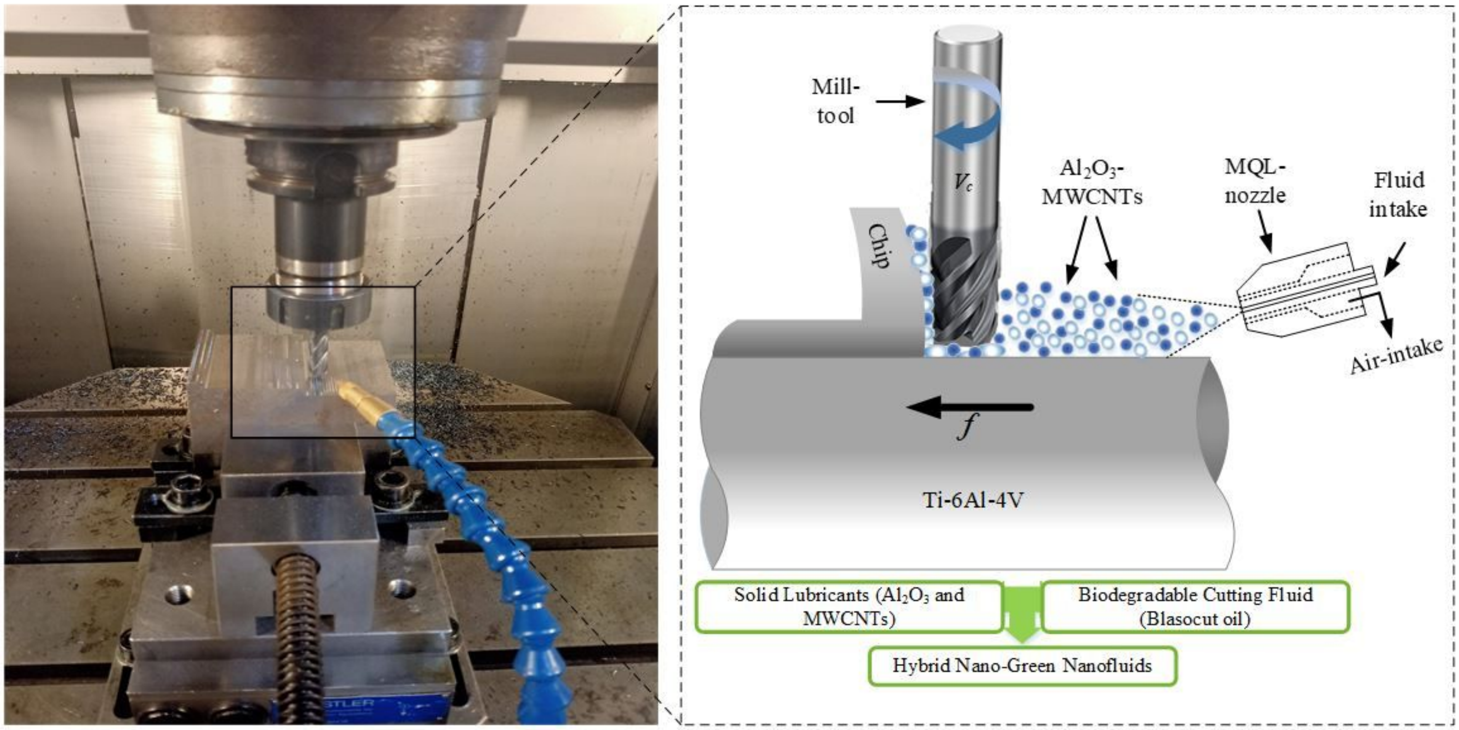

Figure 1

Application of hybrid nanofluids through the minimum quantity lubrication system

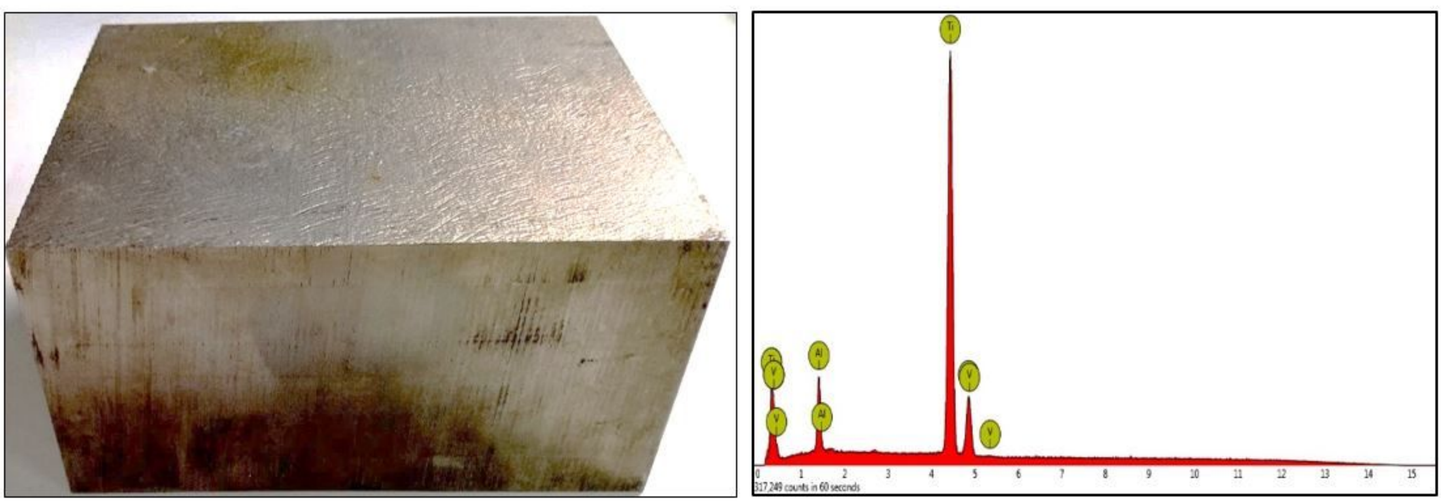

Figure 2

(a) The workpiece sample prepared for milling process (b) EDS analysis of the workpiece

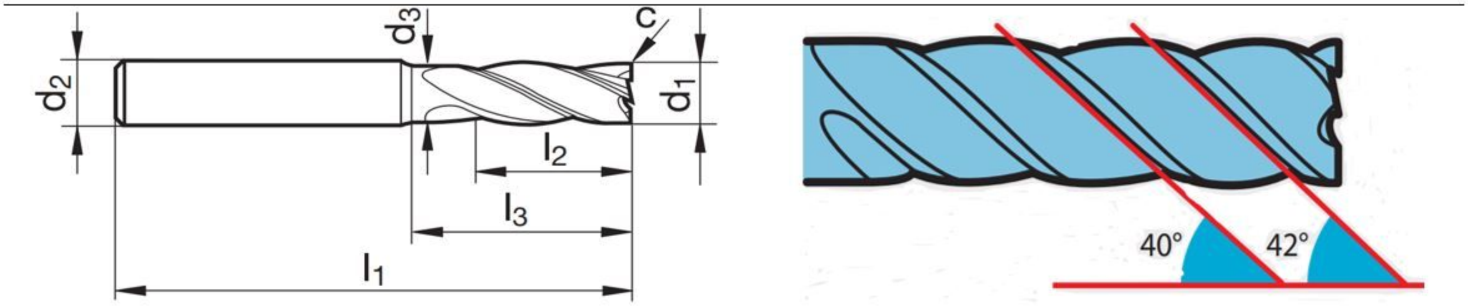

d1(mm) h10	d2(mm) h6	d3(mm)	I_1(mm)	I_2(mm)	I_3(mm)	C(mm×45°)	Z	Ø°	Hardness:
8	8	7.70	63	19.0	26.0	0.15	4	40~42	<1300 N/mm^2

Figure 3

The coated carbide power-mill with geometric characteristics

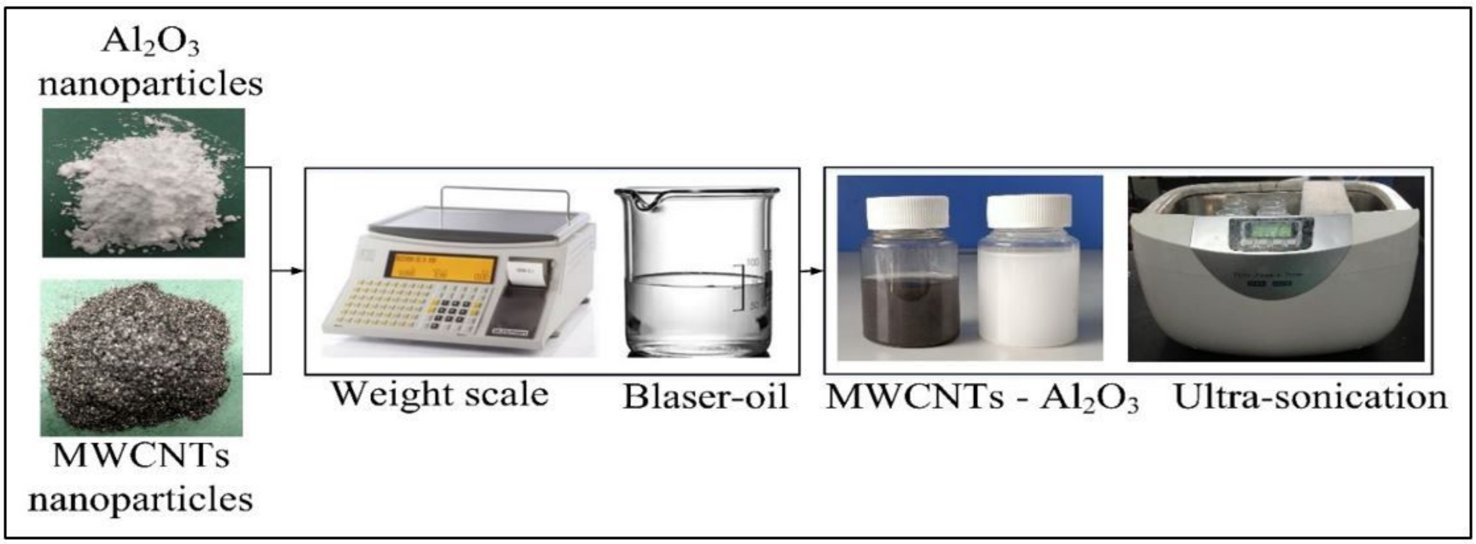

Figure 4

Two-step method to prepare hybrid nanofluids

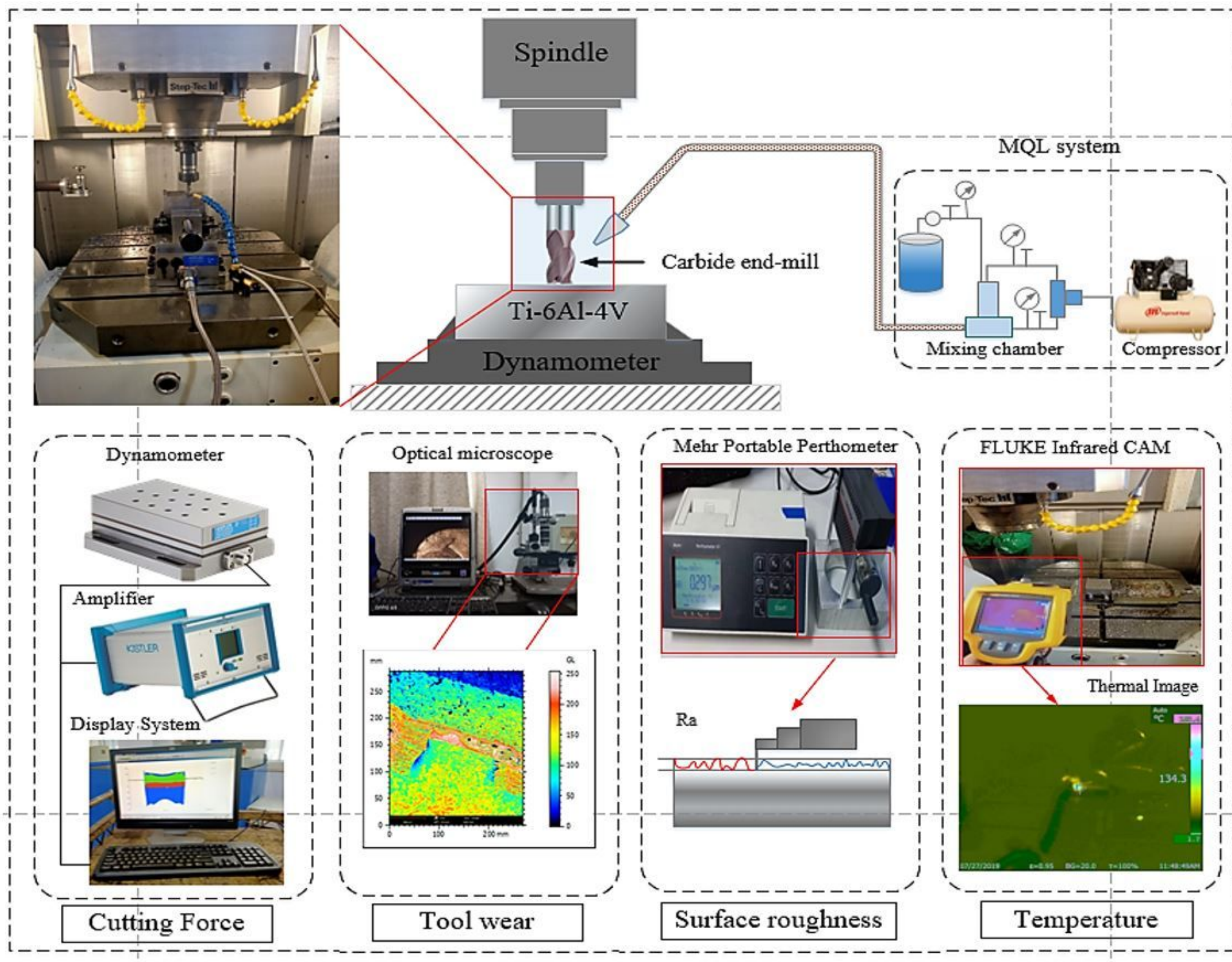

Figure 5

Minimum quantity lubrication system for automatic lubrication

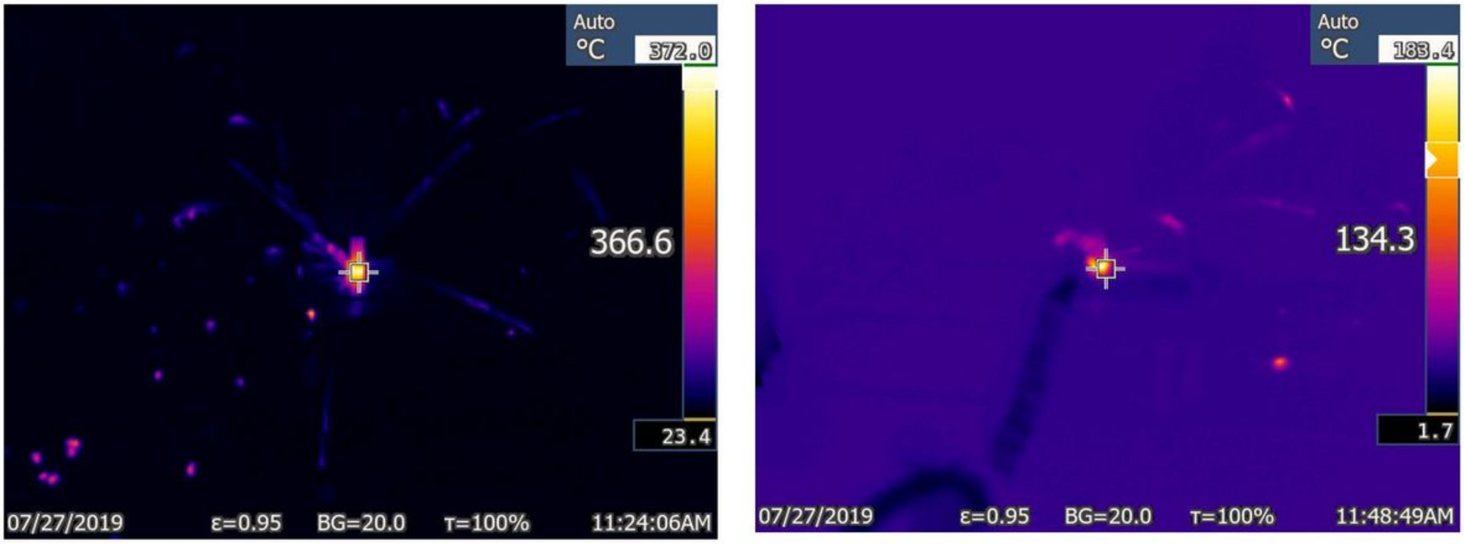

(a) (b)

Figure 6

Temperature under (a) dry and (b) MQL hybrid nanofluids

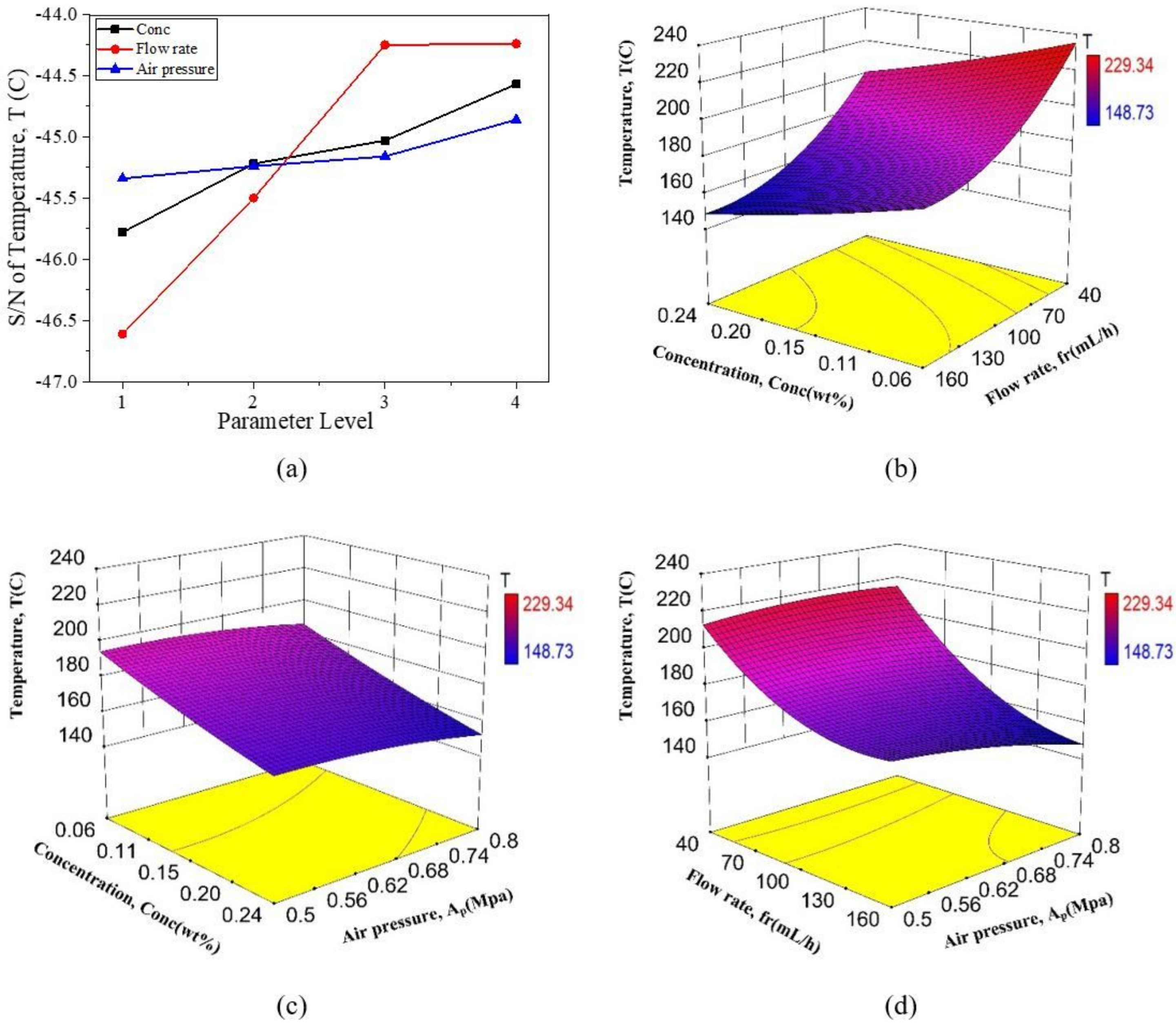

Figure 7

(a) S/N ratio of temperature T, 3D surface plot of (b) Conc (wt%) vs. fr(mL/h) (c) Conc(wt%) vs. Ap (MPa) (d) fr (mL/h) vs. Ap (MPa)

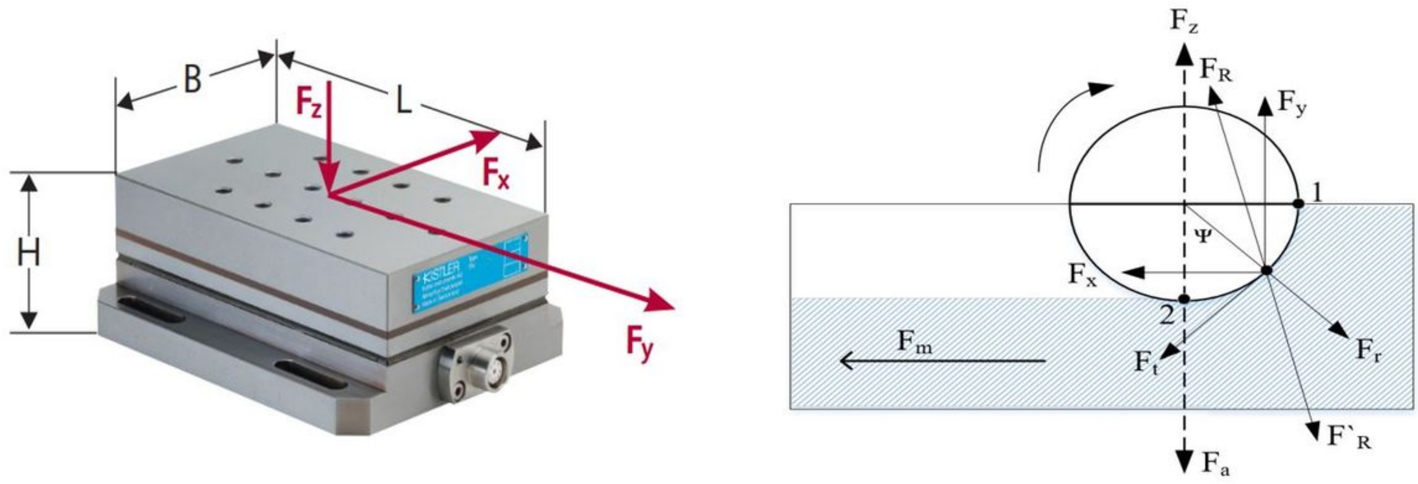

Figure 8

(a) Force components Fx, Fy and Fz on a dynamometer (b) The force components in the milling process [25]

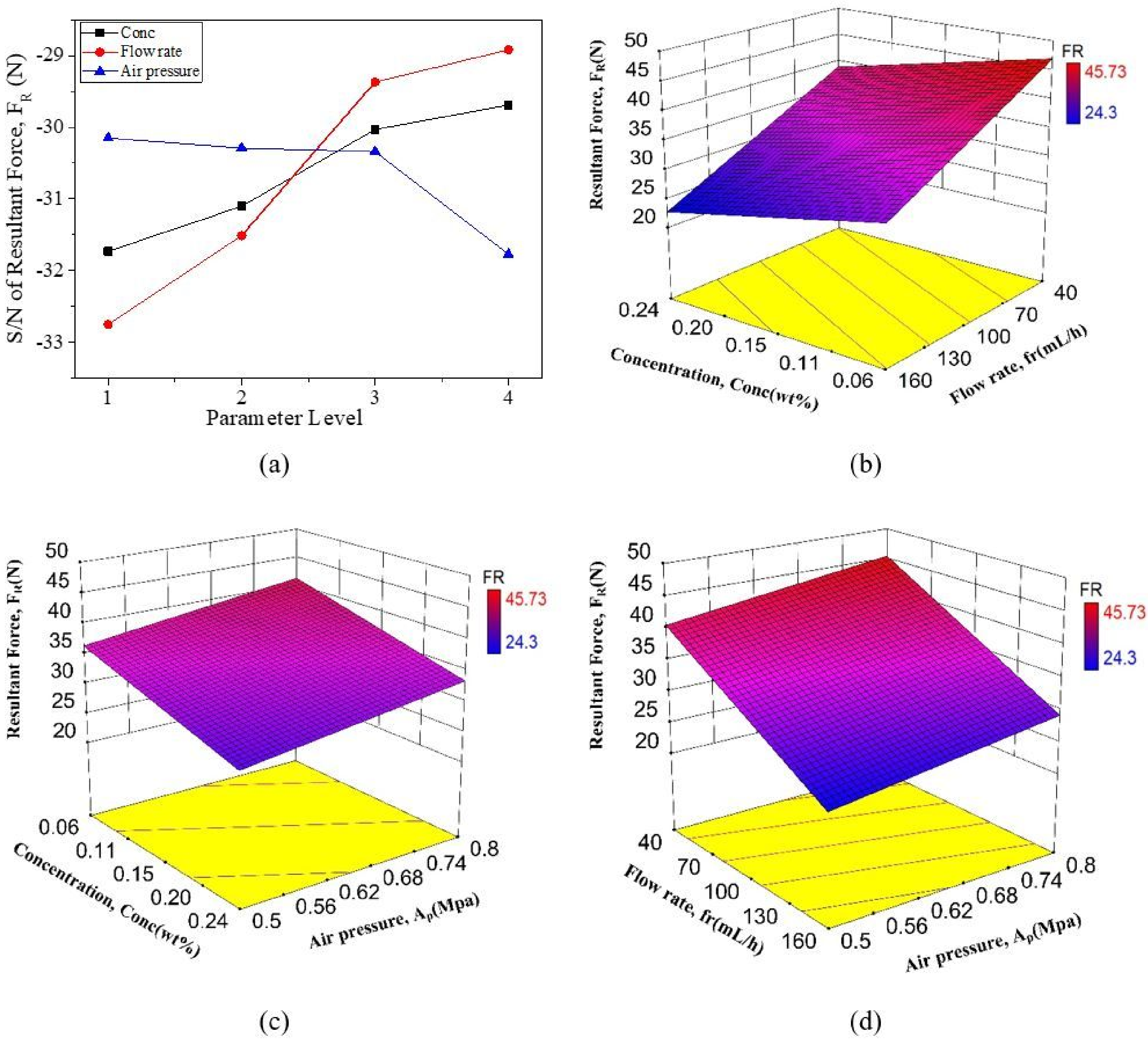

Figure 9

(a) S/N ratio of resultant force FR, 3D surface plot of (b) Conc(wt%) vs. fr(mL/h) (c) Conc(wt%) vs. Ap (MPa) (d) fr(mL/h) vs. Ap (MPa)

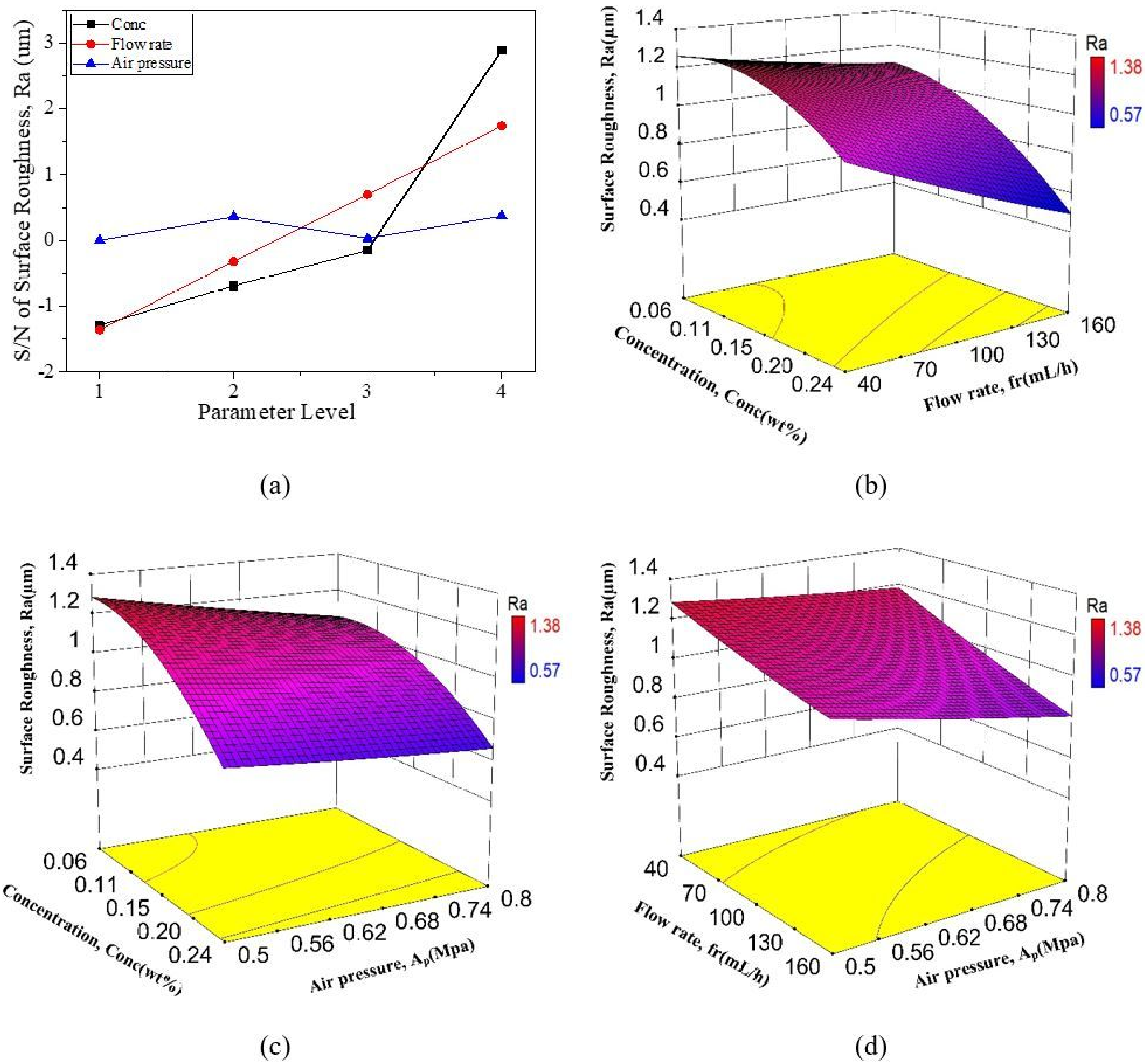

Figure 10

(a) S/N ratio of temperature Ra, 3D surface plot of (b) Conc (wt%) vs. fr (mL/h) (c) Conc (wt%) vs. Ap (MPa) (d) fr (mL/h) vs. Ap (MPa)

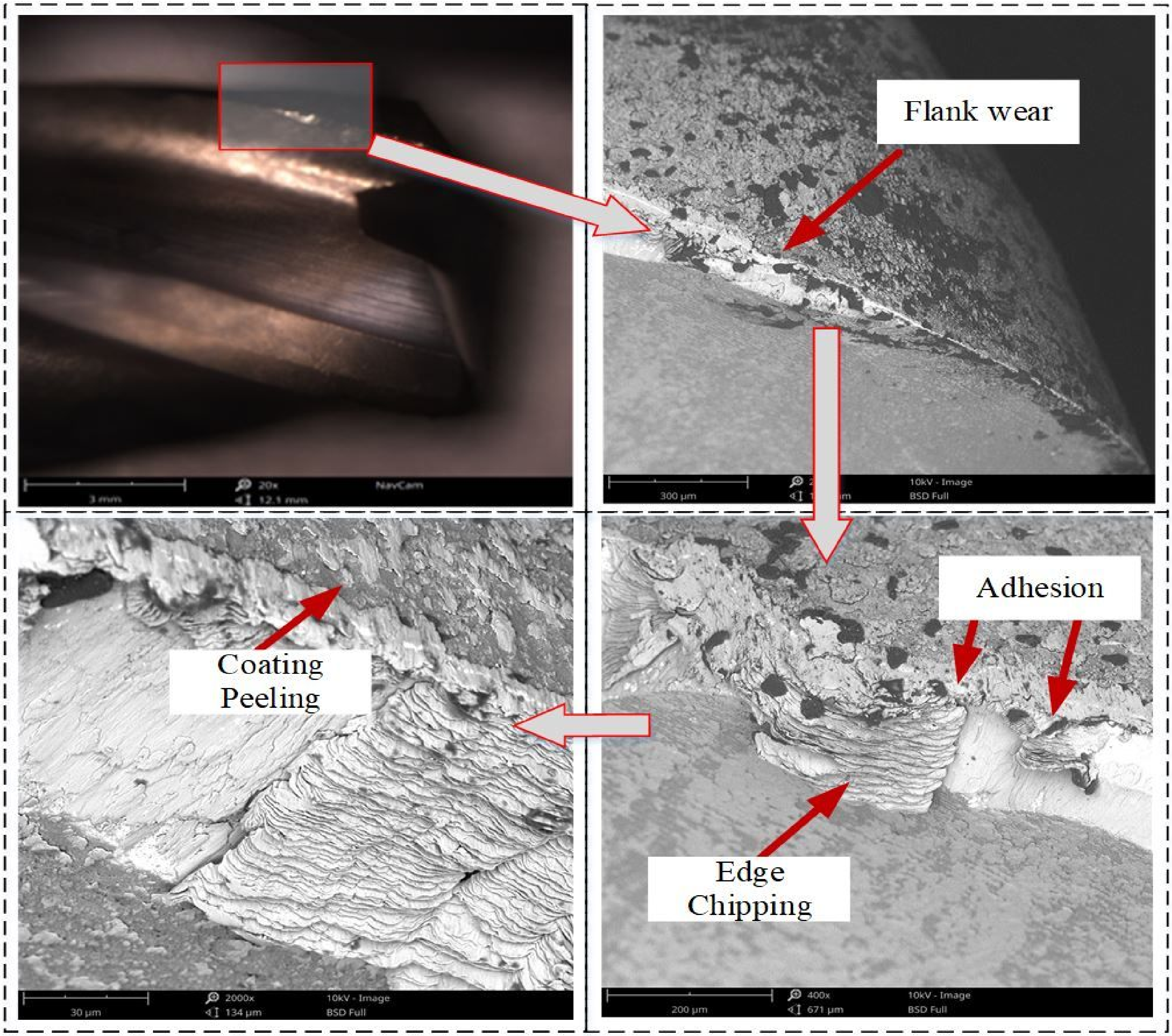

Figure 11

The SEM analysis of the milling tool under 0.24 wt% concentration, 120 mL/h flow rate, and 0.6 MPa air pressure

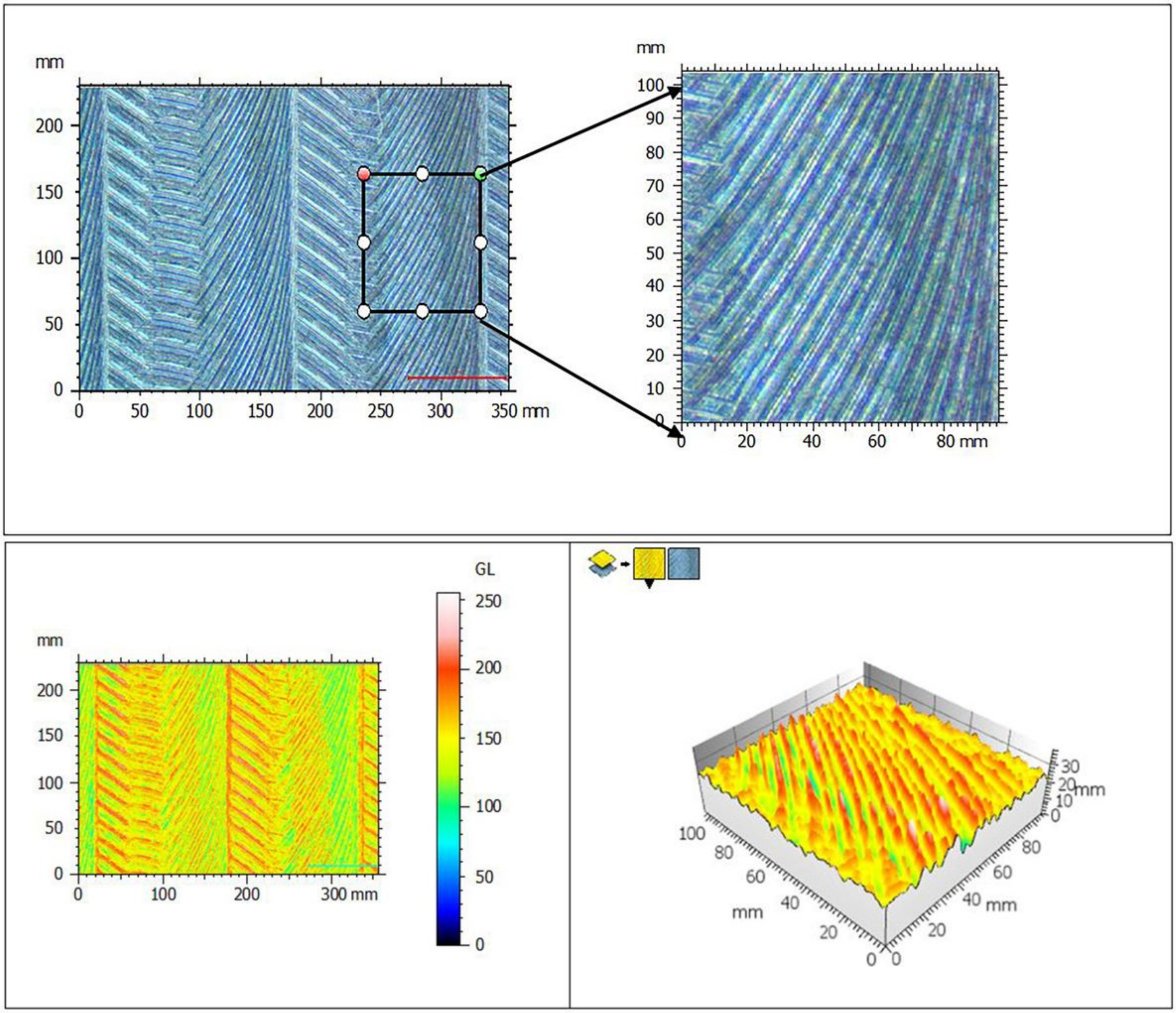

Figure 12

Surface topography of the machined surface at nanofluids concentration of 0.24vol%, 120ml/h of flow rate at 0.6MPa of air pressure

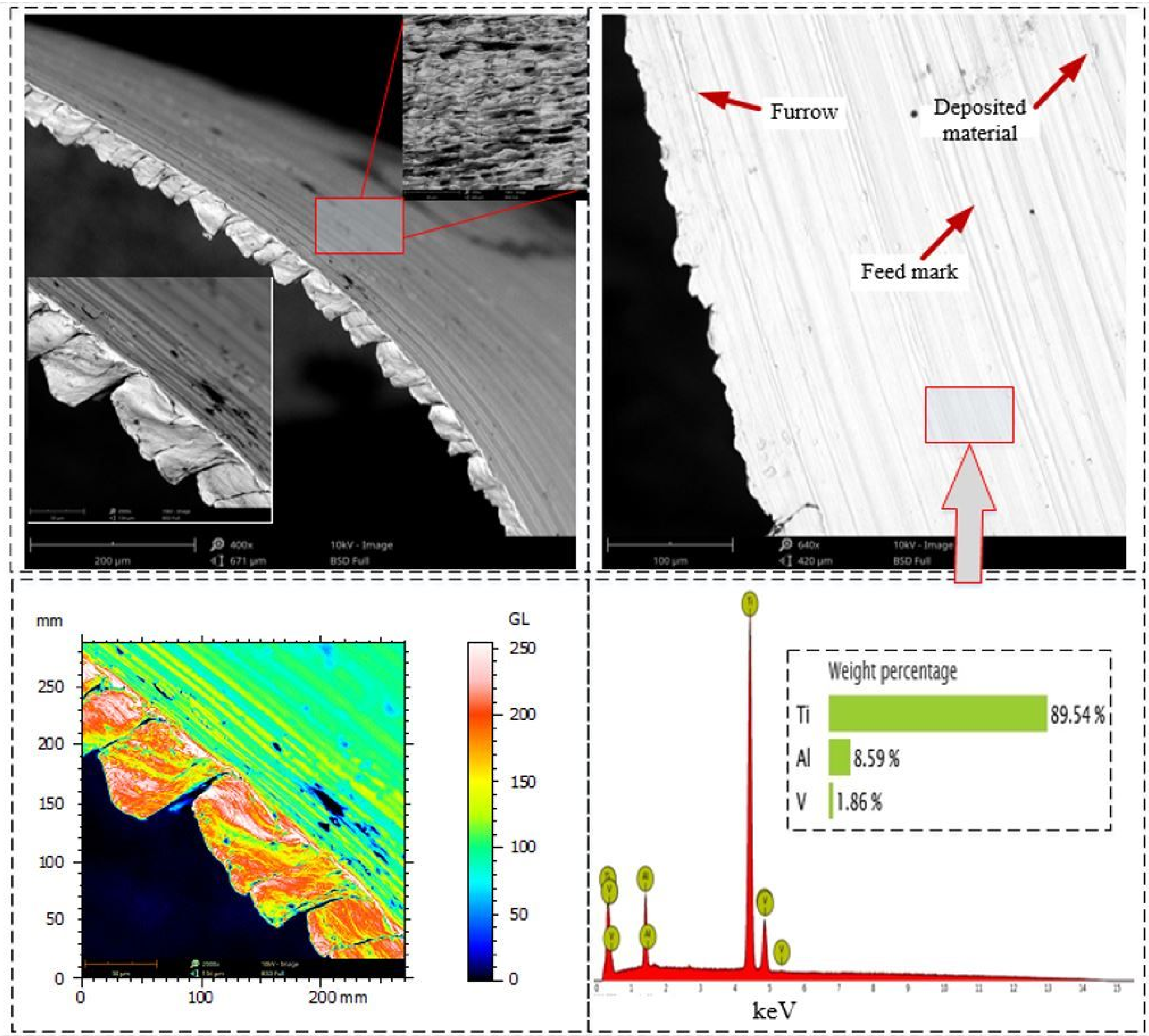

Figure 13

The SEM analysis of chip and EDS of the chip produced under MQL machining at a nanofluids concentration of 0.24vol%, 120ml/h of flow rate at 0.6MPa of air pressure

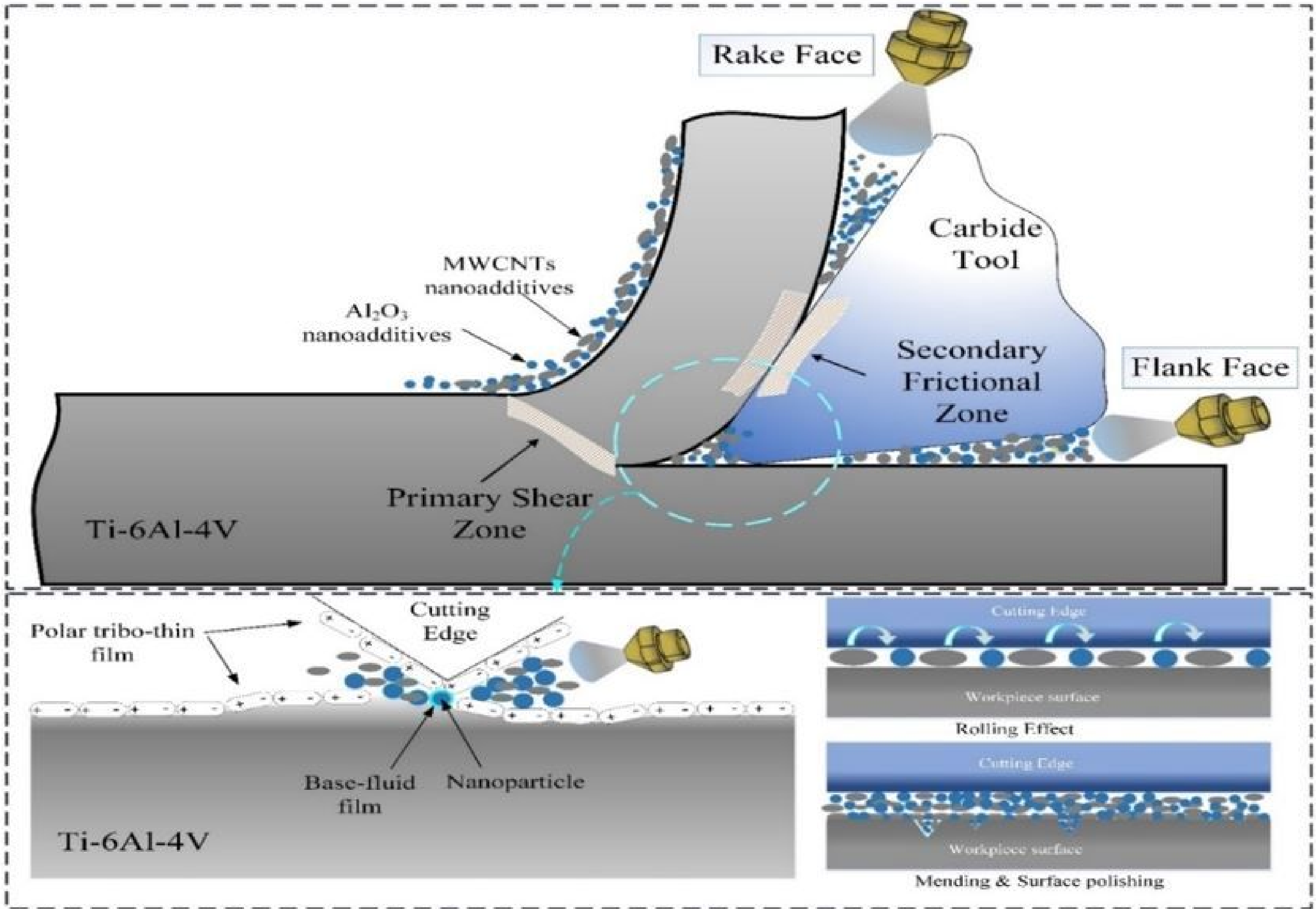

Figure 14

The hybrid nanofluids mechanism and effect on machining Ti-6Al-4V